Galactic Dynamics and the spread of Galactic Civilisations

Markus Strickert

Lund Observatory
Lund University

2020-EXA168

Degree project of 15 higher education credits
June 2020

Supervisors: Anders Johansen and Paul McMillan

Lund Observatory
Box 43
SE-221 00 Lund
Sweden

Abstract

The idea of the spread of life through the galaxy is, in most minds, considered science fiction. Yet, scientists argue that most galaxies have had more than enough time for civilisation development and space travel. In this thesis I simulate how civilisations can spread through the galaxy via close encountering stars, assuming they travel at sub-relativistic speeds. A defined region around the solar neighborhood, populated by Sun-like stars, is simulated over time by tracking the motion of stars using the epicycle approximation. The systems of stars include suitable planets for life development (abiogenesis) where each step of the planet's evolution process is represented by a certain evolution index. The indices are governed by comparing a random number to a probability distribution, representing the probability for a planet to evolve. The probability distribution is in turn extended by including a steepness parameter N, where $N = 0$ gives a Poisson distribution while $N > 1$ produces a distribution that is more tightly peeked. The model keeps track of close encountering stars, which allow for civilisations to colonize a passing, habitable planet. On average, a star's nearest neighbor is at a distance of 36, 47, and 82 pc for simulations with 1000, 600, and 200 stars respectively. By changing the probability distribution that governs the chance of index increase, the first technologically developed civilisation was found after 0.27, 3.65, or 4.8 Gyr, depending on the steepness parameter of the probability distribution. The number of colonized planets over time followed an exponential increase in the beginning with a fall-off close to the saturation point of the number of stars. For star counts of 200, 600, and 1000 stars, allowing only one civilisation to travel while the others remain stationary on their home planets, the galaxy became dominated by the single spreading civilisation only when considering 1000 stars with a steepness parameter of $N = 3$. In this case, 89 per cent of the planets were colonized by the single civilisation. For 200, 600 and 1000 stars and $N = 0$, the stationary civilisations dominated, colonizing 99 %, 99.3 % and 99.7 % of the planets respectively. For $N = 3$, 85 % of the 200 planets and 66 % of the 600 planets were dominated by the stationary civilisations after 12 Gyr. This implies that decreasing the mean distance between stars (by including more stars) in addition to including the steepness parameter, made it possible for a single civilisation to colonize the galaxy faster than the rate of which stationary civilisations develop.

Populärvetenskaplig beskrivning
- Är rymden en enda stor tunnelbana?

Finns det utomjordiskt liv i universum? Konceptet av Fermi paradoxen har förundrat forskare sedan tidigt 50-tal. Den ställer frågan om varför utomjordiskt liv inte har blivit upptäckt ännu. I jämförelse med andra system i universum är vårt solsystem relativt ungt med sina 4,6 miljarder år. Detta betyder att stjärnor med äldre planetsystem bör haft mer än nog tid för en utomjordisk civilisation att sprida sig genom universum. Stuart Armstrong och Anders Sandberg hävdar i ett papper (Armstrong and Sandberg 2013) att kolonisera universum är en "relativt enkel uppgift" för en civilisation med utvecklad teknologi och energikällor rustat för rymdresor.

Men, för möjligheten av utomjordiska resor behövs kunskap kring planetsystem och stjärnors faktiska rörelse samt vilka möjligheter dessa har att utveckla beboeliga förhållanden. Vi vill inte spendera en livstid sökande efter en planet för att tillslut hamna på en planet som Gliese 581c, som skulle - vilket en artikel i Bored Panda (Stella 2019) bildligt beskriver - "smälta dig levande på närsidan och frysa dig till en snögubbe på fjärrsidan".

Trots att rymden är relativt tom finns ändå tonvis av omkringflytande objekt vilket kan påverka stjärnors rörelse och dra dem ur deras banor. Även strukturen av galaxen kan påverka sättet som stjärnorna rör sig. Dessa så kallade "störningar" gör att stjärnor börja vobbla kring sin, i jämvikt, cirkulära bana, vilka tillsammans med stjärnornas rörelse, bildar så kallade epicykelrörelser.

I mitt projekt är målet att simulera spridningen av en civilisation genom en galax likt vår egen. För att lyckas med detta måste en förståelse kring dessa epicykelrörelser skapas. Dessutom, att få en uppfattning om vilka sannolikheter och möjligheter det finns för planeter att skapa beboeliga förhållanden. Genom att skapa ett datorskript, innehållande denna bakomliggande fysik, kan en simulering över spridningen göras. Det slutgiltiga resultatet ger en beskrivning över hur ett sådant datorskript kan byggas upp, samt en illustrativ simulering över spridningen av en eller flera civilisationer genom galaxen.

Så frågan är tillslut: är rymden bara en stor tunnelbana av anslutande spår att resa med? Kan det vara så att dessa spår bara inte är tillräckligt utvecklade ännu och att vår kapacitet inte för tillfället räcker till? Den här simuleringen kan ge insikt i varför vi inte redan nu äter våra middagsmåltider tillsammans med utomjordingar och därtill, ge en uppfattning om när och om den möjligheten någonsin kommer att finnas.

Contents

List of Figures **3**

List of Tables **7**

Acknowledgements **8**

Introduction **9**

1 Galactic Dynamics **11**
1.1 Background 11
1.2 Theory 11
1.2.1 Epicycle approximation 11
1.2.2 Close encounters 14
1.2.3 Simulation setup 14

2 Galactic Civilisations **16**
2.1 Background 16
2.2 Theory 16
2.2.1 Drake's equation and evolution indices 16
2.2.2 Stochastic manipulation 18
2.2.3 Abiogenesis and evolution states 18

3 Algorithm and Method **20**
3.1 Background 20
3.2 Galactic dynamics 20
3.3 Galactic civilisation 21

4 Results **25**
4.1 Background 25
4.2 Galactic dynamics 25
4.3 Galactic civilisations 31

5 Discussions and conclusions **38**

A Animations **42**

B Formal derivation of the epicyclic approximation **47**

Bibliography **49**

List of Figures

4.1 A plot illustrating the radial oscillations for a star in an epicyclic orbit as a function of time, with an oscillating amplitude of ~ 0.7 kpc. . . 26

4.2 A plot illustrating the azimuthal motion of two stars relative to the center of the box. Note the difference between the motion of the two stars. The motion in $R\Delta\phi$ depends on several stochastic parameters (equation 1.16) which makes the outcome of each star unique. Since the motion is seen relative to the center of the moving box, the retrograde motion of one star can be seen as it appears to "turn" along its orbit. 27

4.3 A plot illustrating the vertical oscillation over time for one star. The mean vertical amplitude of oscillation considering 1000 stars is 0.6 kpc, but is, due to the random amplitude b, frequency ν and phaze φ_z different for each star. 27

4.4 A figure displaying the Cartesian motion of one star considering the $x = R\cos(\Delta\phi) - R_0$ and $y = R\sin(\Delta\phi)$ motions in the plane, disregarding any vertical oscillations. Since the motion is relative to the center of the box, at a distance R_0 from the galactic center, the $-R_0$ term is included. Notice that the orbits of stars are also followed outside the box, hence the range on the x-axis is extended compared to the values seen in Table 1.1. 28

4.5 A plot showing the average number of close encounters against the number of iterations per Gyr. The limit distance is set to 10 pc and the relations are shown for 400- up to 1000 stars in steps of 200. The convergence for all numbers of stars tested, occurs at ~ 10000 iterations or equally, a time step of ~ 0.01 Myr with the standard deviation shown as error bars on each of the plots. The standard deviation follows the regular $\sigma = \sqrt{\frac{\sum(x_i - x_{mean})^2}{N}}$ with N denoting the total amount of stars considered. 29

4.6 A figure showing screenshots of 6 iterations for the animation of the epicycle motion of 100 stars. The purpose is to show how the number of close encounters increases over time. In this simulation, 1 time unit = 1 Myr with the blue dots indicating stars that under some iteration had a close encounter. The first close encountering stars are found after $\sim$ 150 Myr and continue to increase over time. Note that the same star can be close to more than one star in the time of the simulation, which explains why there are an uneven number of stars in some screenshots. This is seen in **(b)** where one of the three stars in the first pair created, formed a new close encounter with the third star. 30

4.7 A histogram showing times for the first planet to reach an evolution index E_3. Here, dt is chosen to the optimized value of 1/10000 Gyr (obtained in section 4.2) and the steepness parameter N from equation (2.3) is varied. The times were determined to $\sim$ 270 Myr, $\sim$ 3.65 Gyr and $\sim$ 4.8 Gyr for $N = 0$, $N = 3$ and $N = 1000$ respectively. The simulation was made with 200 stars. 31

4.8 A comparison between the change of evolution indices for 200 stars over 12 Gyr. The blue dash-dotted line shows index 1 stars, the orange dashed line index 2 stars and the filled green index 3 stars. In **(b)**, a steepness parameter of $N = 3$ has been added, giving the characteristic effect of narrowing the spread of indices since the probability distribution becomes more narrow. 32

4.9 Two histograms showing the number of colonized planets per civilisation on the vertical axis and the civilisation number C in rising order on the horizontal axis. Here, $C = 0, 1, 2, 3, ..., n$ where $C = 1$ denotes the first developed civilisation and n stands for the last civilisation to develop on a planet. The left panel depicts this for a steepness parameter $N = 0$ and the right panel $N = 3$. Note that in the case of $N = 3$, the first few developed civilisations dominate while for $N = 0$, there is a more uniform distribution between colonized planets. The simulation is performed considering 1000 stars. 33

4.10 The graph illustrates the fraction of planets colonized when only a single civilisation is able to travel between stars, while the other civilisations stay stationary on their home planets. $N_{\text{spreading}}$ describes the planets colonized by the single civilisation and $N_{\text{stationary}}$ are the planets colonized by stationary civilisations. The left plot displays the fraction for 200, 600 and 1000 stars for steepness parameter $N = 3$ and the right shows this for $N = 0$. Note that if $N_{\text{spreading}}/N_{\text{stationary}} > 1$, the single civilisation dominates. It can be seen that only for 1000 stars with $N = 3$, the single civilisation has colonized more planets than there are planets with stationary civilisations. The convergence seen in the graphs is when there are no more planets to colonize, hence, when every star has reached evolution index 3. Note that the simulation in the right panel begins at time $\sim$ 3 Gyr. This is the time when the first civilisation has developed. 35

4.11 An illustration over the evolution of indices for 200 stars and the colonization of the first developed civilisation. Index 0 stars are seen as red stars, index 1 stars as light blue, index 2 stars as olive green, index 3 stars as navy blue and the colonized stars by one civilisation are seen as red circles. The steepness parameter is set to $N = 0$. The time stamps of the screenshots are chosen to illustrate the times of transition, thus, when most of the stars increase in index. The time step used is $\mathrm{d}t = 2.4$ Myr and the time of the simulation is set to 12 Gyr. 36

4.12 An illustration over the evolution of indices for 200 stars and the colonization of the first developed civilisation. Index 0 stars are seen as red stars, index 1 stars as light blue, index 2 stars as olive green, index 3 stars as navy blue and the colonized stars by one civilisation are seen as red circles. The steepness parameter is set to $N = 3$. The time stamps of the screenshots are chosen to illustrate the times of transition, thus, when most of the stars increase in index. In comparison to figure 4.11, there is very little mixing between the indices. This is a result from the included steepness parameter which narrows the probability distribution, making the chance of index increase small for times smaller than the process times T_{n}. The time step used is $\mathrm{d}t = 2.4$ Myr and the time of the simulation is set to 12 Gyr. 37

A.1 A figure showing screenshots of 6 consecutive iterations for the animation of the epicycle motion of 100 stars. The purpose is to show how stars move in epicycle motion. In this simulation, 1 time unit = 1 Myr with the blue dots indicating stars that under some iteration had a close encounter. Note that the same star can be close to more than one star in the time of the simulation, which explains why there are an uneven number of stars in some screenshots. This is seen in **(b)** where one of the three stars in the first pair created, formed a new close encounter with the third star. 43

A.2 A figure showing screenshots of 6 iterations for the animation of the epicycle motion of 100 stars. The purpose is to show how the number of close encounters increases over time. In this simulation, 1 time unit = 1 Myr with the blue dots indicating stars that under some iteration had a close encounter. The first close encountering stars are found after ~ 150 Myr and continue to increase over time. Note that the same star can be close to more than one star in the time of the simulation, which explains why there are an uneven number of stars in some screenshots. This is seen in **(b)** where one of the three stars in the first pair created, formed a new close encounter with the third star. 44

A.3 An illustration over the evolution of indices for 200 stars and the colonisation of the first developed civilisation. Index 0 stars are seen as red stars, index 1 stars as light blue, index 2 stars as olive green, index 3 stars as navy blue and the colonized stars are seen as red ball shapes. The steepness parameter is set to $N = 0$. The time stamps of the screenshots are chosen to illustrate the times of transition, thus, when most of the stars increase in index. The time step used is $\mathrm{d}t = 2.4$ Myr and the time of the simulation is set to 12 Gyr. 45

A.4 An illustration over the evolution of indices for 200 stars and the colonisation of the first developed civilisation. Index 0 stars are seen as red stars, index 1 stars as light blue, index 2 stars as olive green, index 3 stars as navy blue and the colonized stars are seen as red ball shapes. The steepness parameter is set to $N = 3$. The time stamps of the screenshots are chosen to illustrate the times of transition, thus, when most of the stars increase in index. In comparison to figure 4.11, there is very little mixing between the indices. This is a result from the included steepness parameter which narrows the probability distribution, making the chance of index increase small for times smaller than the process times T_{n}. The time step used is $\mathrm{d}t = 2.4$ Myr and the time of the simulation is set to 12 Gyr. 46

List of Tables

1.1 A table displaying the boundary values for the region around the solar neighborhood in terms of the starting positions in radius R and azimuth angle ϕ. 15

2.1 A table describing the different evolution indices used in the script. Since the spreading of civilisations in general occurs several times, the T_{process} is set to t for index ≥ 2, indicating the different times this happens over the simulation period. 19

4.1 A table showing the average amount of close encounters found over the time of 1 Gyr, depending on the number of stars given. Here, σ_{max} denotes the maximum standard deviation found and f the fraction between close encounters and all possible pairs of stars. 29

Acknowledgements

I would like to express my deepest appreciation to my supervisors Anders Johansen and Paul McMillan who guided me through this project and helped me face difficulties throughout the work. I also wish to thank my fellow bachelor colleagues for discussing and helping me debugging issues regarding the code. Finally, I would like to extend my appreciation to the authors of the Numpy and Scipy packages (Oliphant 2006; Virtanen et al. 2020) whose works have helped me optimize the code used for the project.

Introduction

For centuries, scientists have been trying to solve the conundrum of finding extraterrestrial life in the universe. In the 1950s, the Italian-American physicist Enrico Fermi introduced the famous paradox of why any extraterrestrial life form has not yet visited us, despite knowing the age of the Universe would be enough time for a civilisation to develop modest technology for space travel (Howell 2018). Even nearby galaxies, with typical ages of 10 - 13 Gyr (Nasa 2019) would have more than enough time to develop a civilisation and for them to travel to nearby systems. According to the evolution patterns on Earth, the time it takes for the development of an intelligent civilisation is ~ 4.54 Gyr. For them to be able to colonize stars in the galaxy, they would have to be technological enough for traveling vast distances in space. A "sufficiently technological civilisation" could be, as Kaku (2008, p.158 - 160) describes, a type I civilisation which has the opportunity for sub-relativistic space travel via e.g. mammoth solar sails, which could reach up to half the light velocity driven by powerful lasers located on the moon, or via ramjet fusion, which uses the heavily abundant hydrogen in space to "scoop" its way through the galaxy. If the goal was to travel as fast as possible through the entire galaxy contrary to colonize planets around sun-like stars, it would "only" take an additional 0.65 Myr according to Carroll-Nellenback et al. (2019) when traveling in sub-relativistic speeds.

This project will further explore how spreading to nearby systems could be a possibility by simulating the spread of civilisations through the galaxy, using numerical methods. A limited section (abbreviated "box" or "region") is defined around the solar neighborhood, including a given amount of stars. In this region, the galaxy is assumed to have homogeneous star density in the galactic plane with periodic azimuthal boundaries such that the box moves in the galactic plane, orbiting the galactic center at a distance called the guiding center. The stars inside this box will follow epicyclic motions, oscillating radially, vertically, and in the azimuth. The project aims to track the colonization of suitable planets by one or several space-traveling civilisations in the box, using the true motion of stars and the probabilities for close encountering stars to develop intelligent life. The project compares how altering the probability distribution for life development of planets around suitable stars could make one or several space-traveling civilisations dominant in terms of the number of colonized planets. It also investigates how such planets evolve, depending on if the planets evolve in time scales according to Earth's or according to more randomized time scales. The fundamentals of this project are based on stochastic processes to simulate motions as well as probabilities. Monte Carlo methods will

be implemented to find probability distributions of life development for the systems considered.

Chapter 1

Galactic Dynamics

1.1 Background

This chapter reviews the extension of circular- into non-circular orbits for stars using the epicycle approximation. A nonperturbative motion for a star is circular around the guiding center with a distance R_0 to the galactic center. The guiding center is used as a reference distance and is for this project chosen in the solar neighborhood. Near-circular orbits of stars caused by disturbances from the galactic potential will be derived partly using Taylor expansions around the guiding center, meaning only a limited region around R_0 can be used. Furthermore, the star density of the galaxy is set to be directionally homogeneous in the plane with periodic azimuthal boundaries, meaning that a star moving out of the section instantaneously emerges back on the opposite side. The stars are allowed to move outside the section, both vertically and radially.

1.2 Theory

1.2.1 Epicycle approximation

The epicycle approximation allows a solution for near-circular orbits of stars in three dimensions. The method describes how orbits projected onto the galactic plane can be described as ellipses around the guiding center. Near-circular orbits can be caused by small velocity perturbations in space that disturb orbits of stars. It can also be created directly from the galactic potential, where for example the gravitational field from the spiral arms (called spiral potential) can cause a star to fall towards the centre of gravity when it is in its slowest part of its orbit (apocentre), disturbing its equilibrium orbit (Francis 2009). Studying these motions in a moving reference frame, the stars can sometimes appear to change the direction of their orbit. This is called retrograde motion or epicycles (Cubarsi 2013; Makarov et al. 2004).

For a star in a circular galactic orbit in the solar neighbourhood, the radial distance $R = R_0$, velocity $V = V_0$, angular velocity $\omega_0 = V_0/R_0$ and angular momentum $L_0 = V_0 R_0$ are assumed to be constant and hence, the central attraction balances

the centrifugal force. The central gravitiational force is given by

$$F_{\mathrm{g}}(R) = \frac{V_{\mathrm{c}}(R)^2}{R}, \tag{1.1}$$

where V_{c} is the circular rotation in the galactic plane and R is the radial distance to the center. Inside a homogeneous spherical mass, $F_{\mathrm{g}} \sim R$, while a flat rotation curve yields $F_{\mathrm{g}} \sim R^{-1}$. By introducing the Oort's constant α, this can be approximated as a power law on the form

$$F_{\mathrm{g}}(R) = F_0(R/R_\odot)^\alpha, \tag{1.2}$$

with F_0 describing the force at the sun's distance $R_\odot$, from the galactic centre. In the solar neighborhood, the Oort's constant in equation (1.2) can be found via

$$\alpha = -\frac{3A + B}{A - B}, \tag{1.3}$$

where A and B are coefficients in km/s/kpc describing the shearing motion of the disk around the sun, and the vorticity in the solar neighborhood respectively. The circular motion in cylindrical coordinates for the star follows the motion given in Lindegren (2010) as

$$\begin{cases} R(t) = R_0 \\ \phi(t) = \phi_{\mathrm{c}}(t) \equiv \phi_0 + \omega_0 t \quad , \\ z(t) = z_0 \end{cases} \tag{1.4}$$

where z_0 lies in the plane of the galaxy, ϕ_0 is the starting azimuthal position of the star and ϕ_{c} is the circular azimuthal motion in the galactic plane. For non-circular orbits, the radial distance is a function of time, and the gravitational force can be approximated by

$$F_{\mathrm{g}}(R) = L_0^2 R_0^{-3}(R/R_0)^\alpha, \tag{1.5}$$

where $\alpha \in [-2, 1]$[1] gives information about the local spatial variations of the stars (Olling and Dehnen 2003). For stars close to the solar position, $\alpha \approx -1.2$ (Lindegren 2010). Equation (1.5) is a combination of equation (1.1) and (1.2), where F_0 has been rewritten in terms of the angular momentum $L_0 = V_0 R_0$ as $F_0 = L_0^2 R_0^{-3}$. Since stars in non-circular motions have varying radial distance to the galactic center, R_0 defines the average position of a star, measured in kpc. Additionally, the centrifugal force is described by

$$F_c = L^2 R^{-3}. \tag{1.6}$$

A small perturbation in space[2] can disturb the orbit of a star, making it oscillate around its guiding center. A radial push outwards begins an outward motion of the star ($R > R_0$), however, since the Oort's constant $\alpha \geq -2$, the centrifugal force will decrease more rapidly than the gravitational attraction, making the resulting acceleration, and therefore motion, pointing inwards ($\ddot{R} < 0$)[3]. Note that in this project,

[1] A value $\alpha < -2$ would give negative mass density according to the Poisson equation.

[2] This can be caused by e.g. merging objects that gravitationally pull the star out of its orbit or instabilities in the evolution of the star.

[3] Conversely, an inward push would result in an outward motion where $\ddot{R} > 0$

the orbits are followed assuming these perturbations from the galactic potential has already happened.

Let a star receive a push that makes it oscillate around its guiding center. The radial acceleration with conservation of angular momentum, $R(t)^2\dot{\phi}(t)$, follows

$$\ddot{R}(t) = F_c - F_g = L_0^2 R(t)^{-3} - L_0^2 R_0^{-3}(R(t)/R_0)^{\alpha}, \tag{1.7}$$

where the expanded radial motion due to the perturbation is the addition of an expansion term $|\xi(t)| \ll R_0$, giving the total radial motion to be

$$R(t) = R_0 + \xi(t) = R_0\left(1 + \frac{\xi(t)}{R_0}\right), \tag{1.8}$$

around the galactic center. From the radial acceleration in equation (1.7), inserting the total radial motion yields a differential equation for the expansion term on the form $\ddot{\xi}(t) = -\kappa^2\xi(t)$, with $\kappa = \omega_0(3+\alpha)^{1/2}$ as the angular frequency, with solution

$$\xi(t) = a\sin(\kappa t + \varphi). \tag{1.9}$$

Here, a denotes the amplitude of a harmonic oscillator and φ is the phase. The conservation of angular momentum now yields a solution for the motion in azimuth. By inserting the total radial motion from equation (1.8) in $L_0 = R(t)^2\dot{\phi}(t)$, the motion becomes

$$\phi(t) = \phi_0 + \omega_0 t + \frac{2\omega_0}{R_0\kappa}a\cos(\kappa t + \varphi). \tag{1.10}$$

The vertical motion is described by

$$z = b\cos(\nu t + \varphi_z), \tag{1.11}$$

where ν is the vertical frequency and φ_z the vertical phase. The complete epicycle motion assuming epicyclic approximation is (e.g. Van Den Bosch 2020)

$$\begin{cases} R(t) = R_0 + a\sin(\kappa t + \varphi) \\ \phi(t) = \phi_0 + \omega_0 t + \frac{2\omega_0}{R_0\kappa}a\cos(\kappa t + \varphi) \\ z(t) = b\cos(\nu t + \varphi_z) \end{cases}. \tag{1.12}$$

We derive this more formally in Appendix B. Intuitively, the R and z terms are simple oscillations around the equilibrium orbits at the distance R_0 from the galactic center. The linear term $\omega_0 t$ in the azimuthal motion describes the linear angular motion of a star around the galaxy in addition to its starting position ϕ_0. The coordinate $(R_0, \phi_0 + \omega_0 t)$ is known as the guiding centre of the orbit.

The orbital frequencies ω_0, κ and ν, in units of Gyr^{-1}, are obtained from a linear relation fitted to the Milky Way potential of McMillan (2017) and follows

$$\begin{cases} \omega_0 = 30 - 3.5(R_0 - R_c) \\ \kappa = 42 - 6(R_0 - R_c) \\ \nu = 83 - 12.5(R_0 - R_c) \end{cases}, \tag{1.13}$$

where $R_c = 8$ kpc denotes the distance from the center of the box to the galactic center. Note that the values 30, 42 and 83 have units Gyr^{-1} and 3.5, 6, 12.5 have units $\text{Gyr}^{-1}\text{kpc}^{-1}$. In the epicycle approximation, we only consider frequency terms up to second order and thus, these frequencies are independent on size of orbit. Finally, the velocity in the azimuthal plane $V_\phi = R\dot{\phi}$ obeys

$$V_\phi(t) = R\left(\omega_0 - \frac{2\omega_0}{R_0} a \sin(\kappa t + \varphi)\right). \tag{1.14}$$

1.2.2 Close encounters

The distance between two stars in a 3-dimensional box can be calculated using the Euclidean distance via

$$d(\boldsymbol{p}, \boldsymbol{q}) = \sqrt{\sum_{i=1}^{3} (q_i - p_i)^2}, \tag{1.15}$$

where $\boldsymbol{p}$ and $\boldsymbol{q}$ denote the position in $(R, R\Delta\phi, z)$ of the stars in 3-dimensional Euclidean space. We define the limit distance, r_t, as the maximum distance a civilisation is willing to travel between two stars. If the distance $d(\boldsymbol{p}, \boldsymbol{q}) < r_t$, the stars count as close encounters and the civilisation could potentially[4] travel there. It is important to note that pairs of stars can stay together over a long period of time. But since we do not include star clusters of the mutual gravity of stars, these are much more likely to be close encounters than long lived pairs.

1.2.3 Simulation setup

To find the stars counting as close encounters, a section (or "box") around the solar neighborhood is simulated, including all of the investigated stars. The box has azimuthal motion according to equation (1.16) and the boundaries of the box are periodic in ϕ, yielding the constraint of the star's motion to always be inside the box. Table 1.1 states its different boundary values. The motion of stars, relative to the center of the box R_c is

$$R\Delta\phi = R\big([\phi(t) - \omega_0(R_c)t - \phi_{\min}] \bmod [\phi_{\max} - \phi_{\min}]\big) + \phi_{\min}, \tag{1.16}$$

where $\phi_{\min}$ and $\phi_{\max}$ are defined in Table 1.1 and $\omega_0(R_c) = 30$ Gyr^{-1} is the constant angular motion of the box when orbiting the galactic center. The close encounters will be further used for tracking the spread of civilisations between planets, via these close encounters. The details of how civilisations can spread through the box are described in chapter 2.

Furthermore, the amplitudes a and b, starting positions R_0 and ϕ_0, phases φ and φ_z and orbital frequencies ω, κ and ν (since they depend on R_0) seen in equation (1.12), are randomly chosen for the simulation. By differentiating the radial and vertical motions seen in equation (1.12) we can extract their amplitudes a and b as typical values depending on the radial and vertical velocity dispersion's. Since the motions

[4] If conditions in section 2.2.1 are met.

Table 1.1: A table displaying the boundary values for the region around the solar neighborhood in terms of the starting positions in radius R and azimuth angle ϕ.

	MAX	MIN
R [kpc]	7.5	8.5
ϕ [rad]	-1/12	1/12

are sinusoidal, the average velocities are $\frac{1}{2}\mathrm{d}t/\mathrm{d}R = \frac{1}{\sqrt{2}}a\kappa$ and $\frac{1}{2}\mathrm{d}t/\mathrm{d}z = \frac{1}{\sqrt{2}}b\nu$. The values of the velocity dispersion's[5] are chosen from Aumer and Binney (2009) where $\mathrm{d}t/\mathrm{d}R \equiv V_\mathrm{R} \approx 20$ kpc/Gyr and $\mathrm{d}z/\mathrm{d}t \equiv V_\mathrm{z} \approx 10$ kpc/Gyr.

By solving for a and b, the typical amplitude values used for the motion of stars in the simulation becomes $a = \sqrt{2} \cdot V_\mathrm{R}/\kappa$ and $b = \sqrt{2} \cdot V_\mathrm{z}/\nu$. The amplitudes are furthermore multiplied by a random number, s, from a right-sided Gaussian distribution, thus, chosen as

$$\begin{cases} a = |s\frac{\sqrt{2}V_\mathrm{R}}{\kappa}| \\ \\ b = |s\frac{\sqrt{2}V_\mathrm{z}}{\nu}| \end{cases} . \tag{1.17}$$

The starting positions R_0 and ϕ_0 are likewise randomly chosen within the boundaries of Table 1.1 using Python's `np.random.rand()` command. The phases are chosen by the same procedure as R_0 and ϕ_0 in the interval of $(\varphi, \varphi_\mathrm{z}) \in [0, 2\pi]$. In the vertical direction, we do not consider any boundaries.

The value of the limit distance is set to $r_\mathrm{t} = 10$ pc in the simulation. This value is chosen such that civilisations can travel between stars within the span of their lifetimes. This is in turn based on that civilisations use fusion engines to travel up to 77 per cent of the speed of light (Kaku 2008). At this speed it takes at least 42.4 years to travel this distance. A lower value would be more convenient for the civilisation since it reduces travel times, while a larger value would force them to live their entire lives on a spacecraft. However, increasing the value of the limit distance would indeed increase the number of possible stars that the civilisation can colonize since more stars fall into the category of being close encounters.

[5]To simplify calculations, velocities are expressed in kpc/Gyr. Note that 1 kpc/Gyr $\simeq$ 1 km/s.

Chapter 2

Galactic Civilisations

2.1 Background

This chapter extends the theory introduced in chapter 1. It uses the dynamics of stars in the box to track the spreading of civilisations through the galaxy. The distances between the stars inside the box are mapped over the time of the simulation and checked for a certain limit distance, called r_{t}. Every star has an evolution index representing the evolutionary states of an orbiting planet, suitable for life development. The indices are based on Drake's equation (2.1) and properly defined in section 2.2.3. A civilisation can arise on a planet that supports the necessities for intelligent life. It can then spread to other planets that have developed habitable conditions. Pseudo-random numbers are generated for every star at every time step which work as switches between the different indices. This will indicate the state of the star-system as well as determine which system the civilisation can travel to.

2.2 Theory

2.2.1 Drake's equation and evolution indices

According to Frank Drake (SETI 2020), an estimation over the number of technological civilisations existing in the universe is based on several probability factors. The number of civilisations N, able to communicate their existence in our galaxy can be estimated with

$$N = R_b T, \tag{2.1}$$

where R_{b} describes the rate of broadcasting civilisations that arise per unit time in the galaxy and T the time interval of broadcasting. Note that T depends on the survival time of the civilisation and the time that the civilisation can continuously broadcast. The R_{b} component is divided into several sub-factors, describing different stages for a suitable star to form a planet with a broadcasting civilisation. The complete equation is commonly written as

$$R_{\mathrm{b}} = R p_{\mathrm{p}} n_{\mathrm{E}} p_{\mathrm{l}} p_{\mathrm{i}} p_{\mathrm{c}}, \tag{2.2}$$

stating that the rate of emergence of new broadcasting civilisations is equal to the suitable stars forming per unit time multiplied by the average mean number of civilizations communicating per star. The different parameters are defined as

$$\begin{cases} R = \text{Rate of stars suitable for life development to form} \\ p_{\mathrm{p}} = \text{Probability of formation of planets around a suitable star} \\ n_{\mathrm{E}} = \text{Average number of suitable planets located in the habitable zone, per planetary system} \\ p_{\mathrm{l}} = \text{Probability of life appearing on such a planet} \\ p_{\mathrm{i}} = \text{Probability for intelligent life to develop on such a planet} \\ p_{\mathrm{c}} = \text{Probability for the civilization to broadcast across space} \end{cases}$$

Note that the formation of a suitable planet requires the host star to have sufficient metallicity, preferably in the range [Fe/H], $\in [-1, 0.5]$ (Zackrisson et al. 2016). The peak formation probability for terrestrial planets to form is [Fe/H] ≈ -1 according to this model. Formally, a star with too low metallicity, [Fe/H] $\lesssim -2$, does not have the heavy elements required (above He) for Earth-like planets to form. Since these heavier elements were not formed as a result of the Big Bang, these are instead produced via nucleosynthesis (Anand et al. 2018; Jones 2019) inside the stars. Lineweaver (2001) describes a "Goldilocks selection effect", where a too low metallicity makes Earth-like planets unable to form, while too high metallicities increase the chance of the formation of giant planets, which in early stages can destroy the formation of smaller Earth-like planets. A comparison between three different models for the probabilities of terrestrial planet formation depending on the host stars metallicity can be seen in Fig. 1 in Zackrisson et al. (2016). This could be used to extend the project in terms of making a comparison for how different planets evolve, depending on the metallicity of their host star. Note, however, that in the simulation used in this project, we assume all stars to be sun-like with metallicities [Fe/H] $\simeq 0$.

The parameters in focus are p_{l} and p_{i} which we represent by four evolution indices. Assume that all stars are solar like, with suitable planets surrounding them, hence, factors p_{p} and n_{E} equals 1. Also assume a civilisation located on a habitable planet (later referred to as an evolution index 3 planet) inside the galaxy. The civilisation is technologically developed (a Type I civilisation in the description of Kaku 2008) and is able to travel to nearby stars within the lifetime of an average human with an assumed limit distance of $r_{\mathrm{t}} = 10$ pc. Based on p_{l} and p_{i}, four evolution indices are defined as E_{n} with $n = 0, 1, 2, 3$, describing the state of evolution for the planet around a star. At the start of the simulation, the stars begin at evolution index E_0. At each time step, the probability for an evolution index to increase by one is $P(E_n \to E_{n+1}) = \mathrm{d}t/T_{\mathrm{process}}$, where $\mathrm{d}t$ is the time step, T_{process} is the mean time for the evolution index to increase by one and $\mathrm{d}t/T_{\mathrm{process}}$ is on the form of a Poisson distribution. The average times and definitions of the evolution indices are presented in Table 2.1.

Furthermore, random numbers are generated each time step which work as switches between the indices. The random numbers (written as R_{N}), are chosen from a

uniform distribution using Python's `Random` package[1]. If $R_{\mathrm{N}} < \mathrm{d}t/T_{\mathrm{process}}$, the index will increase one step and the planet evolves. The conditions $n \geq 2$ and the distance $d < r_{\mathrm{t}}$ must be fulfilled in the targeted star for the civilisation to be able to spread there, since a lower evolution index would make the planet impossible to inhabit and a larger distance too far away.

2.2.2 Stochastic manipulation

The evolution indices are based on letting the random number R_{N} become smaller than a certain value $\mathrm{d}t/T_{\mathrm{process}}$ which corresponds to a Poisson distribution on the form, $P(t) = e^{-\lambda(t-t_0)}$. Here λ is a rate parameter and $t - t_0$ is the time since the beginning of the simulation. Generally, the probability for this is low since the time step $\mathrm{d}t \ll T_{\mathrm{process}}$. Regardless, using many number of iterations makes the indices increase and reach the final index 3 state, even for small $t - t_0$. We can manipulate this to make the evolutionary processes (the increase of indices) of planets to match the evolutionary processes on Earth, where Earth's process times can be seen in Table 2.1. To match these evolution processes, we make the probability for $R_{\mathrm{N}} < \mathrm{d}t/T_{\mathrm{process}}$ become larger in the limit where the time since the last index increase approaches T_{process}. An extension of the Poisson distribution, in terms of equation (2.3), increases this probability as $t_{n-1} \longrightarrow T_{\mathrm{process}}$ and follows

$$P(E_n \to E_{n+1}) = \frac{\mathrm{d}t}{T_n} \left(\frac{t_{n-1}}{T_n} \right)^N , \tag{2.3}$$

where $T_n = T_{\mathrm{process}}$ with $n = 0, 1, 2, 3$ representing the different evolution indices, t_{n-1} is the time since arriving at previous evolution index and N is a steepness parameter. Note that for $N = 0$, the Poisson distribution is returned. For $N > 0$ and $T_n \gg t_{n-1}$, the probability for an evolution index increase is small, but increases as $t_{n-1} \longrightarrow T_n$. By increasing N, the "boosting" of the probabilities can be altered, since it steepens the probability distribution. Hence, the factor N can be manipulated such that the indices E_n are reached in correspondence with the values in Table 2.1. For all scenarios we consider, $P(E_{\mathrm{n}} \to E_{n+1})$ is small.

Note that a small value of N represents the evolution of a planet that deviates in its evolutionary patterns compared to Earth while a large N makes the planet evolve in coherence Earth's time scales. The steepness parameter can therefore be used to compare how planets evolve if we assume that planets evolves similar to an Earth-like planet or differently. This could also be achieved by changing the T_{process} values in Table 2.1 such that it matches the desired way of planetary evolution.

2.2.3 Abiogenesis and evolution states

Abiogenesis describes the theory that organisms can arise spontaneously from inanimate matter and is the basis for the assumed T_{process} in the model. According to

[1]Note that these numbers are not truly random but instead called pseudo-random numbers. These are generated using deterministic processes. More information about pseudo-random numbers can be found in Kennedy (2020)

Table 2.1: A table describing the different evolution indices used in the script. Since the spreading of civilisations in general occurs several times, the T_{process} is set to t for index ≥ 2, indicating the different times this happens over the simulation period.

Index	**Description**	**Colour**	**Shape**	T_{process} [Gyr]
0	A suitable planet in the habitable zone	Red	star	-
1	Life development	Cyan	star	0.3
2	Habitable conditions for a civilisation*	Olive green	star	3.5
3	Intelligent life	Navy blue	star	0.7
$\geq$2	Close encountering star with habitable conditions	Red	circle	t

*The habitable conditions are based on that a stable oxygen level has been maintained on the planet such that a civilisation can live there without any extra equipment.

the model in Spiegel and Turner (2011), the probability per unit time λ for life to develop around a suitable star within its lifetime in the main sequence ($t_{\text{min}} = 0$ and $t_{\text{max}} \leq 10$ Gyr)[2] is given by a Poisson distribution. This means life must evolve within the interval $t \in [t_{\text{min}}, t_{\text{max}}]$ and that life occurs from a single process (as an on/off switch) despite it probably being far more complex. This model states that life arose at least once (and begun the process of life development) 3.8 billion years ago (Ga), with an uncertainty of a few hundred million years. In comparison, the paper of Dodd et al. (2017), claims that the first life form might have arisen earlier. They have compared filament tubes found in seafloor hydrothermal vents with microfossils living in younger rocks. The consistency in the comparison yielded the promising results that biological activity in these seafloor vents could have been active up to almost 4.3 Ga. This means that life might have arisen without the need for oxygen and that organisms thrived on other energy sources, such as the chemical reactions close to a hydrothermal vent via chemosynthesis (Anand et al. 2018). However, for more complex life to exist, sufficient oxygen levels seem to be of main importance. The current level of oxygen in our atmosphere is a direct by-product of the photosynthesis of cyanobacteria which according to Canfield et al. (2000) reached its current level between 0.54 - 1.0 Ga.

The algorithm used for the probability of evolution index increase is based on the on/off model from a Poisson distribution and is more firmly described in section 3.3. The life development time follows the claims of Dodd et al. (2017) with the oxygen development time in the interval given by Canfield et al. (2000). The third evolution index is based on the "rest" time, which all added should equal the age of Earth ($\sim$ 4.5 Gyr). Note that, in reality, there could be overlap between the processes. Although the first life form emerged around 300 million years after the formation of Earth, the process of oxygen development might not have occurred until several hundreds of million years after. But the simulation requires fixed times for the processes to work as switches between indices and thus, the potential overlap is unconsidered.

[2]For Sun-like stars.

Chapter 3

Algorithm and Method

3.1 Background

In this chapter, the general algorithms are described in terms of pseudo-codes. The algorithm will be divided into two parts:

1. Galactic dynamics and close encounters
2. Abiogenises using Monte Carlo methods (called "Galactic civilisation"),

where the first aims to describe the script setup for the epicycle motion of stars around the solar neighborhood inside the defined box. The second part aims towards simulating life-developing processes for close encountering stars regarding:

- Life development
- Oxygen development
- Technological civilisations.

Note that the algorithm is based on generating pseudo-random numbers using Python's `np.random.rand()`. This means that each time the script is run, a new outcome of the result is obtained. To get equal results each time, the seed of the random number generators can be set to some value by using the `random.seed()` command in the beginning of the simulation. This is only needed if it is desired to get the same output each time the code is run (Kennedy 2020).

3.2 Galactic dynamics

The dynamics of stars follow the equations found in section 1.2.1, with the equations of motion seen in equation (1.12). The code aims to introduce a certain amount of stars, measured in the frame of the galaxy, that move in the also moving box around the solar neighborhood, having periodic boundaries in the azimuth. The starting position of stars, R_0 and ϕ_0, phases φ and φ_z and amplitudes a and b are randomly selected in their intervals (stated in section 1.2.3) with the latter two

taken from a right-sided Gaussian distribution. The Euclidean distances between the stars are calculated for each time step over the given amount of time. A limit distance is set to define close encounters and the pairs of close encounters are put in a specific list. Note that gravity between stars is neglected throughout the simulation. The final code can plot the oscillations in R, ϕ and z, find all close encounters for every iteration throughout the given amount of time, animate the motion of stars in Cartesian coordinates and plot the convergence of the number of iterations needed such that no close encounters are disregarded.

A pseudo-code for this can be described as

1. Define a function `starmotion` depending on the number of stars, time and the number of iterations used. This function will return desired plots and values in the end.
2. Define lists to include the motions in R, ϕ, z, x and y and set a limit distance called `tolerranceradius` for close encounters (10 pc for this specific project).
3. Define the boundaries of the box as in Table 1.1.
4. Optional*: To get the same result every time the script runs, include a seed value using the command `np.random.seed(x)`, for a fixed integer value x.
5. Define the random parameters using `np.random.rand()` for the starting position of all stars and `np.random.normal()` for the amplitudes. Also define the orbital frequencies seen in equation (1.13).
6. Create a list of all possible pairs of stars, named `pairlist,` on the form: $(1,2),(1,3),...(2,3),(2,4),...,(i,j)$ of length $N_\mathrm{s}(N_\mathrm{s}-1)/2$, for the number of stars N_s. These pairs will be matched with the close encountering stars in `starlist`, defined in point 8.
7. For N_s stars over all iterations, loop over the equations for R, z and $R\Delta\phi$ in equations (1.12) and (1.16) respectively and insert their positions in a list called `totalist` on the form $\mathbf{A}_i = [[R_i, z_i, R_i\Delta\phi_i]]$, where i denotes the star considered.
8. Calculate the euclidean distance between all stars over all iterations inside the loop using the command `np.pdist` and insert the stars whose distances are smaller than the `tolerranceradius`, r_t, in a new list called `starlist`. Empty the list after each step to save memory and return the wished list. `pairlist` is used here to keep track of which stars that will be inserted in `starlist`.
9. Run the function for some amount of `stars`, `time` and `iterations`.

3.3 Galactic civilisation

The method is based on the Drake equation, seen in equation (2.1). The code will determine which stars are considered habitable or not, using indices called evolution indices. The meaning of each index can be seen in Table 2.1. A pseudo-random num-

ber is generated each iteration and compared to the probabilities of index increase, described in section 2.2.1. If the random number is smaller than this probability, the index increases by one. The first star to reach an evolution index of three represents the first planet with an intelligent civilisation. This star is checked for all close encountering stars with an evolution index of two. If the two close encountering stars follow those requirements, the civilisation can spread. Over time, as more planets develop intelligent civilisations, the same procedure is done on all these planets to track the spreading of every civilisation through the galaxy.

The code can output the evolution indices of each star and a list over the spread of stars in tuples on the form (x, y) where the civilisation travels from star x to y at time t. Furthermore, the process can be animated in the 2D Cartesian plane representing the plane of the galaxy around its guiding center. The stars change color depending on their current evolution index and symbol if their planet is colonized according to the colors and symbols in Table 2.1. Furthermore, the code can be used to check to what extent the box becomes dominated by a single spreading civilisation in comparison to multiple stationary civilisations that stay on their home planets. It can also be used to investigate how this fraction depends on the number of stars given and how the fraction changes when varying the steepness parameter.

1. Optional*: To get the same result every time the script runs, include a seed value using the command `np.random.seed(x)`, for a fixed integer value x.

2. Create a list, equally long as the number of stars given and generate a pseudo-random number for each position in the list. The command can be `np.random.rand(N)`, for N_s stars.

3. Loop this list over all iterations and give the probability after each iteration for a star to increase its current evolution index. The probability is given by $\mathrm{d}t/T_\mathrm{process}$ where $\mathrm{d}t$ is the time step and T_process is the average time it takes for the planet to increase its evolution index by one. Put these in a separate list called `indexlist`. Append the stars with indices 1, 2 and 3 in three different lists.

4. Loop over the evolution indices and use different probabilities between the different evolution indices from Table 2.1. If the random number $R_N < \mathrm{d}t/T_\mathrm{process}$, increase the index by one.

5. Define a variable `found=False`. Append the first star with evolution index 3 into a list and change `found=True`. Also define a new list `spread_stars` which colonized stars are to be appended in.

6. Loop over all the close encountering pairs obtained in the `starlist` from section 3.2. If `found=True` and if the star checked is in `spread_stars`, append it into a list called `habitablelist`. Check if the 0:th position of the pair of stars is not in `spread_stars`, if so, reverse the pair of stars to get the right order (inhabited star in 0:th position in tuple travels to 1:st position in the tuple) and append into `habitablelist`. Also constrain this to only be valid for stars with E_n where $n = 2$ for the conditions to be met. Repeat the same

procedure for the 1:th position in the pair of stars.

7. For comparison, check the difference of the spreading of civilisations if the planets instead use the probability distribution seen in equation (2.3), thus, if the planets evolve in coherence to an Earth-like planet, redo the simulation but change the probability $\mathrm{d}t/T_{\text{process}}$ to the distribution in equation (2.3) and vary the value of N. The larger the N, the narrower the distribution will be and the more the transition times between indices will happen according to the process times of Earth.

To measure the fraction of colonized planets by a single spreading civilisation compared to the number of planets naturally developing a civilisation, the following pseudo-code can be used:

1. Define a list called `civindex` with length of the number of stars considered, consisting of zeros. Define a variable called `civcount` and set it to zero outside the time loop. Also define a list called `index3list` which keeps track of the stars that have reached an evolution index of three.

2. Loop through `index3list`. If a star reaches index 3 and is not already in that list, append that star into the list. At the same time, increase `civcount` by one and append that into `civindex`. Now, if e.g. star number 53 is the first star to reach an evolution index of three, this is put as the first item in `index3list`. Since we know that it is star number 53 that was the first star to reach this index, `civindex` will have a value one in position 53 in the list. The next star value appended into `index3list` will put a value of two in that star value position in `civindex`. In this way, every star becomes unique, with its value governed by the `civcount`.

3. Check if the first civilisation found already is in `spread_stars`. If it is not, it means that the civilisation on that star will spread to the 1:st position of its pair from `starlist`. Put these now colonized stars in `civindex` . This will put values of "ones" in the position of the planets colonized by the single spreading civilisation in `civindex`.

4. Check the number of stars colonized by the first civilisation (hence, the number of "ones" in `civindex`) divided by the rest of the index 3 stars that the first civilisation has not colonized (the values that are not "ones" in `civindex`) in every iteration and plot against time. Also, test this for varying steepness parameter $N = 0$ and $N = 3$ for 200, 600 and 1000 stars.

The packages used for the code and animations are

```
import numpy as np
import matplotlib.pyplot as plt
import matplotlib.animation as animation
from array import *
import random
from scipy import *
from scipy.spatial.distance import pdist
```

```
from matplotlib import cm, colors, pyplot as plt
from IPython.display import HTML
import copy
import ffmpeg
```

Chapter 4

Results

4.1 Background

This chapter presents the results obtained from the simulations made in chapter 3 along with brief discussions. The first part quantifies and displays the oscillation magnitudes from the epicycle motions for a simulation time of 1 Gyr together with the Cartesian motion of one star in the galactic plane. It also shows the results of finding the convergence parameter dt with a supplied table describing properties about close encountering stars. Lastly, results from the animation of close encountering stars are shown together with six illustrative screenshots.

The second part states the time it takes for the first star to reach an evolution index of three, depending on the change of the steepness parameter N from section 2.2.2. The realism of these times is briefly discussed in comparison to the evolutionary patterns on Earth. The change of evolution index when allowing all civilisations to spread can also be seen. Finally, only the first developed civilisation was allowed to spread and colonize index 2 planets in the galaxy. The rest of the civilisations developing around index 3 stars stay stationary at their home planets. The fraction between colonized planets by the single traveling civilisation and the planets colonized by the stationary civilisations are measured over time, depending on the steepness parameter N and the number of stars considered.

4.2 Galactic dynamics

Figure 4.1 displays the radial oscillation for a star around the equilibrium orbit R_0 where the total radial oscillation magnitude is ~ 0.7 kpc. Since the starting positions R_0, phase φ, and amplitude a is chosen randomly within the boundaries, the oscillation magnitude will be different for each star. The average magnitude of oscillation for 1000 stars is $R \approx 1.1$ kpc over 1 Gyr. Note that the oscillation does not change over time since we follow stars motion in the galactic potential, assuming perturbations from the potential have already happened.

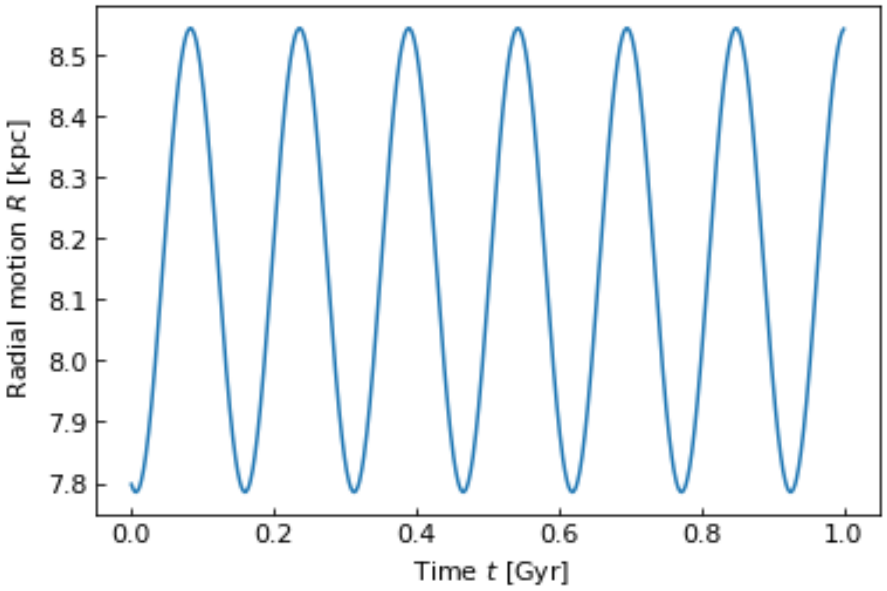

Figure 4.1: A plot illustrating the radial oscillations for a star in an epicyclic orbit as a function of time, with an oscillating amplitude of ~ 0.7 kpc.

The azimuthal motion, described by $R\Delta\phi(t)$ in equation (1.16), is depicted in Figure 4.2. The motion describes the box of stars moving linearly with $\omega_0 t$ through space with the oscillating motion of the stars relative to the center of the box. Since $R\Delta\phi$ depends on several stochastic parameters, the resulting motion of each star is different. Note that the motion of the box itself is for convenience since the stars would be moving quickly through the box otherwise. The mean value of azimuthal motion relative to the center of the box is 1.4 kpc.

Figure 4.3 shows the vertical motion for one star inside the box. The star oscillates around the galactic plane with a mean magnitude of 0.6 kpc. Also here, the randomly chosen amplitude b and frequency ν yields different outcomes for each star. It can be seen that stars on average tend to oscillate more vertically then radially, thus, that the frequency ν is larger than κ. Since each of the orbital frequencies ω, κ and ν depends on R_0, it is indeed in correspondence with equation (1.13) that $\nu > \kappa$ for a star starting at position R_0.

The motion in Cartesian coordinates is shown in Figure 4.4 for one star. Each star moves in unique patterns inside the box which is illustrated in the animation screenshots in Figure A.1 in Appendix A. The motion becomes complex since it oscillates in each direction but is simplified in the screenshots where we disregard any vertical motions. The resulting motion in (R, ϕ) follows retrograde motion in an ellipse with prograde motion in its guiding center. Retrograde motion[1] can make stellar objects appear to stop and move backward under some time in a moving reference frame. In the case of this simulation, since the motion of stars is relative

[1] An example is Earth- and Mars's orbit relative to each other. Since Earth orbits approximately two times as fast as Mars, mapping the tangential line of sight position of Mars in orbit gives an illusion of Mars stopping and moving backwards relative to Earth at certain times.

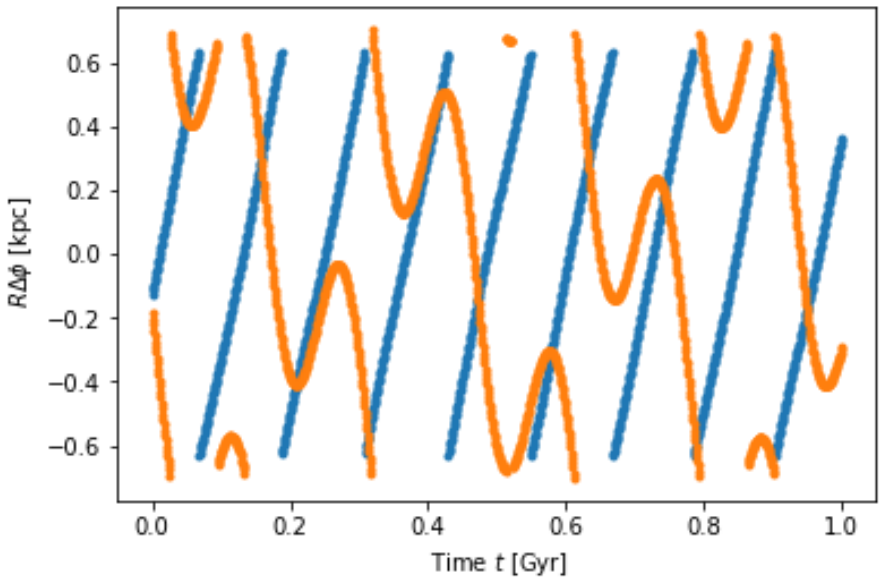

Figure 4.2: A plot illustrating the azimuthal motion of two stars relative to the center of the box. Note the difference between the motion of the two stars. The motion in $R\Delta\phi$ depends on several stochastic parameters (equation 1.16) which makes the outcome of each star unique. Since the motion is seen relative to the center of the moving box, the retrograde motion of one star can be seen as it appears to "turn" along its orbit.

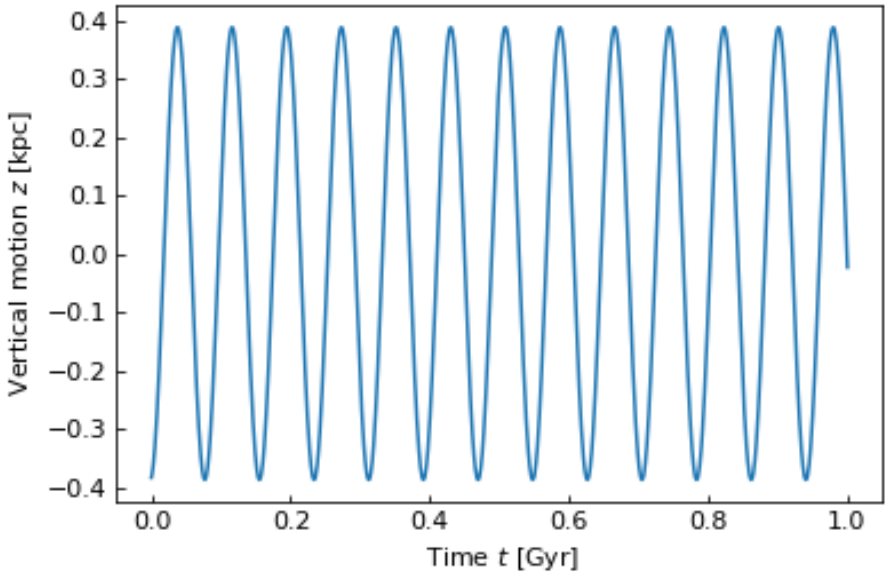

Figure 4.3: A plot illustrating the vertical oscillation over time for one star. The mean vertical amplitude of oscillation considering 1000 stars is 0.6 kpc, but is, due to the random amplitude b, frequency ν and phaze φ_z different for each star.

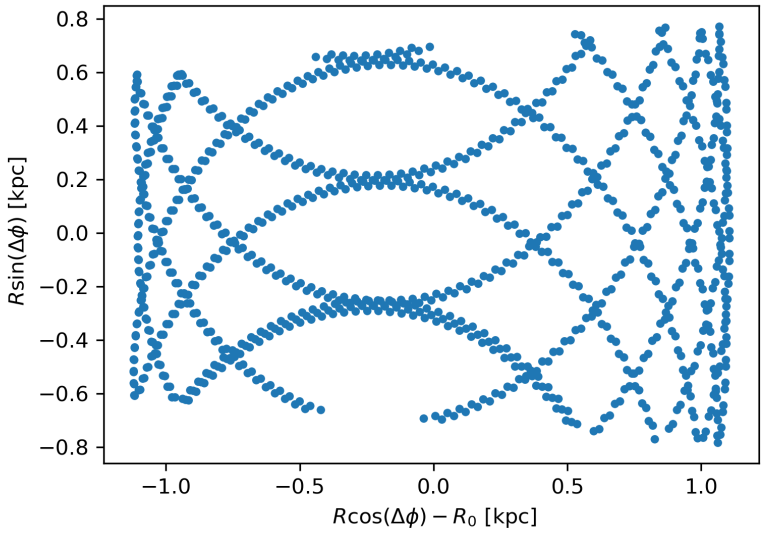

Figure 4.4: A figure displaying the Cartesian motion of one star considering the $x = R\cos(\Delta\phi) - R_0$ and $y = R\sin(\Delta\phi)$ motions in the plane, disregarding any vertical oscillations. Since the motion is relative to the center of the box, at a distance R_0 from the galactic center, the $-R_0$ term is included. Notice that the orbits of stars are also followed outside the box, hence the range on the x-axis is extended compared to the values seen in Table 1.1.

to the center of the moving box, the stars sometimes appear to have this motion. If the orbital angular momentum vector of the object is in the opposite direction compared to the orbit, it is called prograde motion of its guiding center (Van Den Bosch 2020).

It is important to note the assumption made when tracing the orbits of stars in this simulation. By increasing simulation time (as done in section 4.3), the motion of stars can change. Here we assume that the epicycle motion of stars are non-changing over time as they move in the galactic potential. As the galaxy evolves, many phenomena can affect the motion of the included stars. This could be e.g merging with other galaxies which can cause stripping effects, changing the orbits of the stars or gravitational perturbations, which could alter the oscillating motions.

By increasing the number density of stars considered, the number of close encounters increases. Table 4.1 displays the maximum amount of close encounters found running the code four times for each star count with a limit radius of 10 pc. The convergence can be seen in Figure 4.5 plotting the average number of close encounters[2] as a function of the number of time steps used over the fixed time of 1 Gyr. The standard deviations can be seen as vertical lines for the different curves and are calculated for each number of stars in Table 4.1. Moreover, the table also states the fraction between all close encounters found and the total amount of possible pairs of stars, $f = N_{\text{close}}/N_{\text{possible}}$, where $N_{\text{possible}} = N(N-1)/2$, denoting stars as N. This fraction

[2]Formally, the mean value of the number of close encounters for all iterations, run four times.

Table 4.1: A table showing the average amount of close encounters found over the time of 1 Gyr, depending on the number of stars given. Here, $\sigma_{\max}$ denotes the maximum standard deviation found and f the fraction between close encounters and all possible pairs of stars.

Stars	**Ave. Close encounters for 50 000 iterations**	$\sigma_{\max}$	f
400	516	±8.3 %	0.6 %
600	1148	±6.2 %	0.6 %
800	2012	±4.7 %	0.6 %
1000	3113	±4.5 %	0.6 %

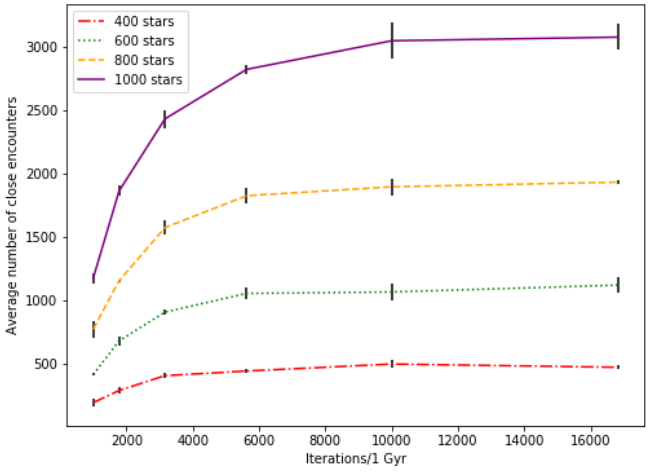

Figure 4.5: A plot showing the average number of close encounters against the number of iterations per Gyr. The limit distance is set to 10 pc and the relations are shown for 400- up to 1000 stars in steps of 200. The convergence for all numbers of stars tested, occurs at $\sim$ 10000 iterations or equally, a time step of $\sim$ 0.01 Myr with the standard deviation shown as error bars on each of the plots. The standard deviation follows the regular $\sigma = \sqrt{\frac{\sum(x_{\mathrm{i}}-x_{\mathrm{mean}})^2}{N}}$ with N denoting the total amount of stars considered.

is the same for the different star counts which means that the number of iterations tested, is enough to find every close encountering pair. Since close encounters of two pairs of stars rarely happen more than one time per Gyr[3], the few pairs that do are neglected.

Finally, the mean distance between the close encounters was determined to be 7.6 pc. The average distance between the stars in general was 82, 47 and 36 pc for 200, 600 and 1000 stars respectively. Assuming Sun-like stars, with velocities according to V_ϕ in equation (1.14), the average velocity was $V_\phi(t) \approx 237$ kpc/Gyr. This yields a centripetal acceleration between the stars, using equation (1.1), of order $2 \cdot 10^{-7}$ kpc/Gyr^2.

[3]Two pairs of stars can be closer than the limit distance many times over some adjacent iterations but is then only counted once. They can also encounter each other more than one time over the full time and those encounters are the ones that are neglected.

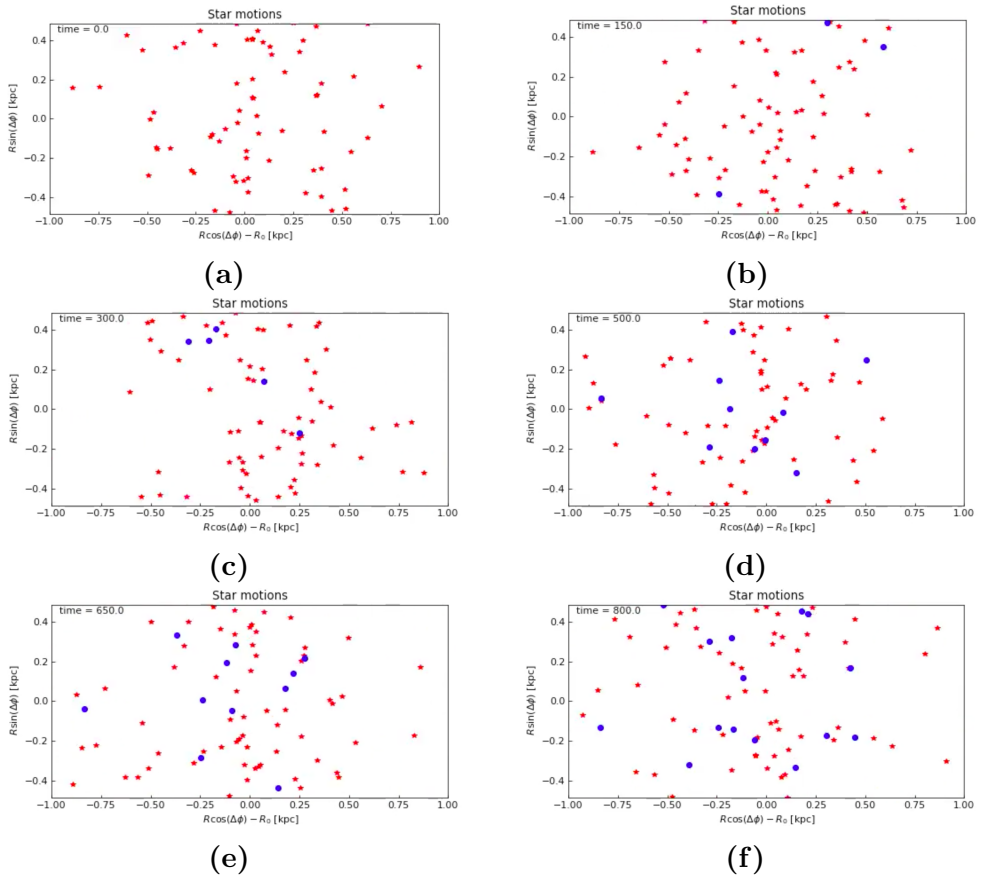

Figure 4.6: A figure showing screenshots of 6 iterations for the animation of the epicycle motion of 100 stars. The purpose is to show how the number of close encounters increases over time. In this simulation, 1 time unit = 1 Myr with the blue dots indicating stars that under some iteration had a close encounter. The first close encountering stars are found after $\sim$ 150 Myr and continue to increase over time. Note that the same star can be close to more than one star in the time of the simulation, which explains why there are an uneven number of stars in some screenshots. This is seen in **(b)** where one of the three stars in the first pair created, formed a new close encounter with the third star.

Screenshots of the animation made from section 3.2 can be seen in Figure 4.6. The six figures indicate how the number of close encounters increases with time. The limit distance r_t is set to 10 pc and the blue circles represent any two stars that at some point in time have been closer than r_t. Each time frame represents 1 Myr and the simulation is run over 1 Gyr. After 800 Myr, 14 close encountering stars had been recorded, with the first ones appearing at the 150 Myr mark. The time step is not set to be optimized throughout this animation due to computing limitations. Nevertheless, it demonstrates how the number of close encounters increases with time. The full animation can be found in the links in Appendix A.

4.3 Galactic civilisations

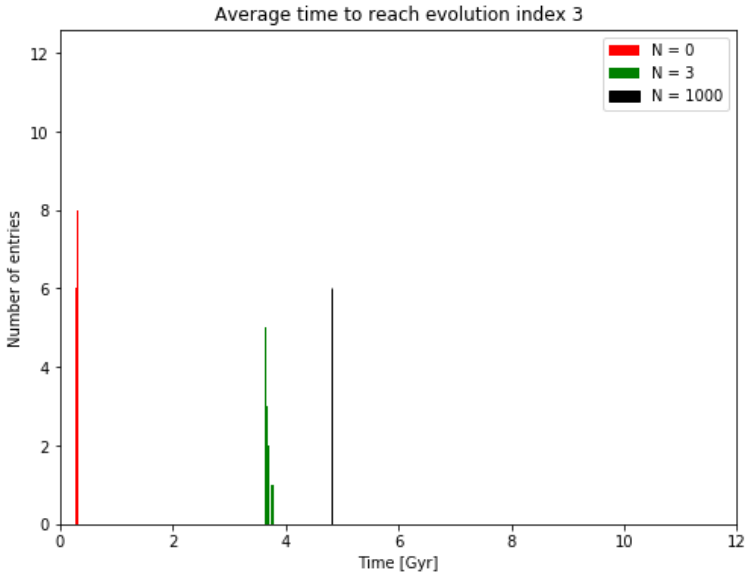

Figure 4.7: A histogram showing times for the first planet to reach an evolution index E_3. Here, dt is chosen to the optimized value of 1/10000 Gyr (obtained in section 4.2) and the steepness parameter N from equation (2.3) is varied. The times were determined to $\sim$ 270 Myr, $\sim$ 3.65 Gyr and $\sim$ 4.8 Gyr for $N = 0$, $N = 3$ and $N = 1000$ respectively. The simulation was made with 200 stars.

For the convergence parameters d$t = 10^{-4}$ Gyr, the average time it takes for the first planet to develop intelligent life, hence have an evolution index E_3 is shown in Figure 4.7. For $N = 0$, the first intelligent civilisation developed after $\sim$ 270 Myr. The short time is due to the broadness of the Poisson distribution when neglecting the steepness parameter. An expected value would be $\sim$ 4.5 Gyr for all the necessary life developing processes to have occurred, if the evolutionary time scales happen according to the ones on Earth.

The extended probability distribution gave results more coherent with the process times in Table 2.1. For $N = 3$, the average time to reach E_3 was $\sim$ 3.65 Gyr and for $N = 1000$, 4.8 Gyr. Compared to an Earth-like planet, $N = 1000$ seems the most reasonable as it compares to the evolution times for such a planet. However, we want the model to vary somewhat in time scales in comparison to Earth. The $N = 3$ model seems to do this, since the time scales is similar to the ones on Earth, but still leaves room for "unusual events[4]" to occur. Since the only known planet to have developed life is Earth, its time scales are considered most reasonable. Nonetheless, other planets could have different processes for the development of life which in term could alter the process times significantly.

Figure 4.8.a shows the development of evolution indices for 200 stars over 12 Gyr. Comparing the results to Table 2.1, there is clear correspondence. The process time

[4]Evolution time scales that are unlike the ones on Earth

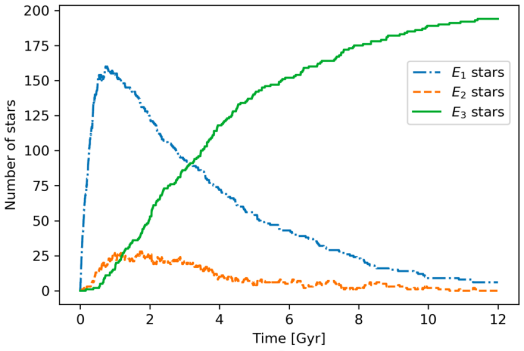

(a) The change in evolution indices over 12 Gyrs for 200 stars when allowing every civilisation to spread between stars. The simulation is made with time step $\mathrm{d}t = 10^{-4}$ and steepness parameter $N = 0$.

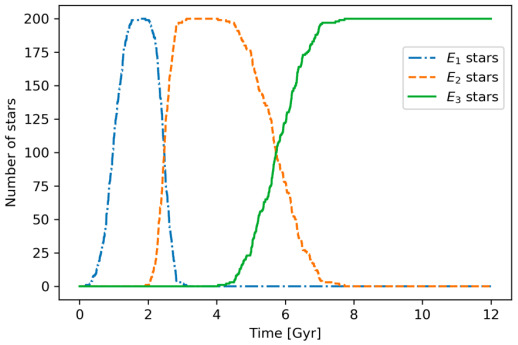

(b) The change in evolution indices over 12 Gyrs for 200 stars when allowing every civilisation to spread between stars. The simulation is made with timestep $\mathrm{d}t = 10^{-4}$ and steepness parameter $N = 3$.

Figure 4.8: A comparison between the change of evolution indices for 200 stars over 12 Gyr. The blue dash-dotted line shows index 1 stars, the orange dashed line index 2 stars and the filled green index 3 stars. In **(b)**, a steepness parameter of $N = 3$ has been added, giving the characteristic effect of narrowing the spread of indices since the probability distribution becomes more narrow.

for $E_0 \to E_1$ is small, formally, 0.3 Gyr, meaning most of the stars will reach this value soon after the start of the simulation. By ~ 1 Gyr, index 1 stars reach their maximum with a few index 2 and 3 stars. The small peak for index 2 stars is a direct result of $\mathrm{d}t/T_{\text{process}}$ being much smaller than for the other indices. Due to the large T_{process}, the jump from $E_1 \to E_2$ requires the random number, $R_{\text{N}} < 2.85 \cdot 10^{-5}$ compared to $P(E_0 \to E_1) = 3.3 \cdot 10^{-4}$ and $P(E_2 \to E_3) = 1.4 \cdot 10^{-4}$. This implies the low peak of the index 2 stars identified in the graph in addition to the fast increase of index 3 stars as soon as the index 2 and index 1 stars starts to reduce. The few index 2 stars are also a result of the colonization of those planets. Since index two stars can either be colonized by a civilisation or jump up in index naturally over time, the index 2 stars start to decrease quickly as soon as index 3 stars begin to dominate. The results also show that disregarding the steepness parameter yields a larger "mix" of planets with different indices over time.

When adding the steepness parameter $N = 3$ from equation (2.3), the indices increase in a less random sense. The narrower distribution allow the indices to stay in their current states longer, since the probability $P(E_n \to E_{n+1})$ is small for small values of t_{n-1}. This can be seen in Figure 4.8.b where every star have reached E_1 before any of them have jumped to E_2. As time reaches ~ 1.8 Gyr, the probability for index increase is around $R_{\text{N}} < 3.5 \cdot 10^{-6}$ and increases for larger t_{n-1}, where the first index 2 stars are seen. The first index 3 stars are found after ~ 3.8 Gyr. The difference in steepness between Figure **(a)** compared to **(b)** represents the value of N. For $N \gg 1$, every star would jump up (or down) in index at the same time since t_{n-1} would have to be extremely close to T_n for the evolution index to increase.

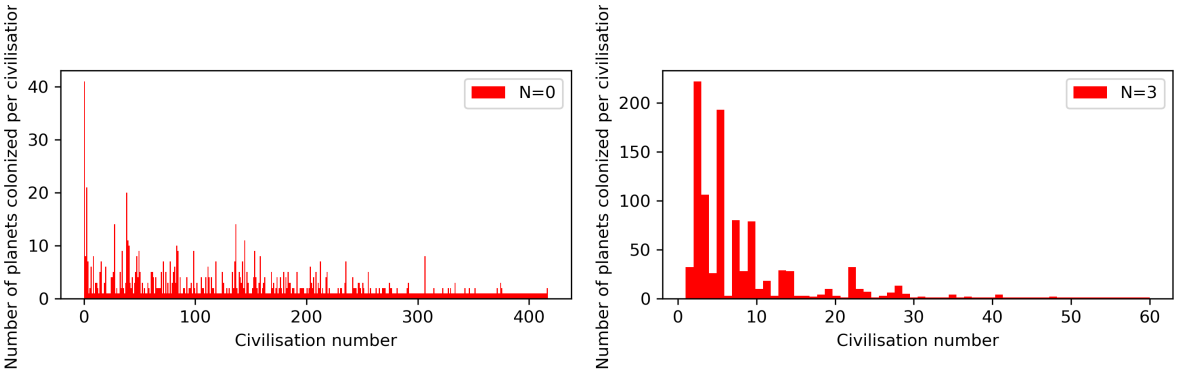

Figure 4.9: Two histograms showing the number of colonized planets per civilisation on the vertical axis and the civilisation number C in rising order on the horizontal axis. Here, $C = 0, 1, 2, 3, ..., n$ where $C = 1$ denotes the first developed civilisation and n stands for the last civilisation to develop on a planet. The left panel depicts this for a steepness parameter $N = 0$ and the right panel $N = 3$. Note that in the case of $N = 3$, the first few developed civilisations dominate while for $N = 0$, there is a more uniform distribution between colonized planets. The simulation is performed considering 1000 stars.

Since we can trace which civilization colonized which planet[5], we can also examine the advantage of early development over late development, in terms of how many planets each civilisation have colonized. Note that each civilization is allowed to spread to planets around the index 2 stars, but once a planet has been colonized, another civilization cannot spread there[6]. Figure 4.9 shows how many planets each civilisation has colonized as a function of its civilization number C. The civilisation number increases sequentially, with $C = 1$ being the first civilisation to develop (hence, for the planet to reach index 3) and $C = n$ being the last civilisation to develop. The maximum number of colonized planets, $n_{\max}$, is the number of stars considered and is set to 1000 in this case. If $C = 0$, it means that this star has neither reached index 3 nor has it been colonized. Studying both cases for the inclusion and exclusion of the steepness parameter N, the second developed civilisation colonized most planets with 21 planets for $N = 0$ and 222 planets for $N = 3$. For $N = 0$ it should be noted that over 400 civilisations either evolved naturally on their planet or also spread to other planets. Because of the broadness of the Poisson distribution, the time interval in which index 2 stars are available for colonization is considerably longer than if the steepness parameter is included. However, they count only a few at each time step, since the indices change their values more randomly. This means that index 2 stars are still available for colonization, even when the late civilisations develop. Note, however, that most of the late developed civilisations have only colonized one planet, the planet on which they evolved.

[5]Since they all have a certain value defined in "civindex" in section 3.3

[6]Conversely, once a civilisation has colonized a planet, it immediately jumps up to index 3. Therefore there cannot be two civilisations on the same planet simultaneously.

For $N = 3$ the transition times between indices are exceedingly narrower which means that indices stay in their current states longer (formally, they stay in their states for time $t \approx T_{\mathrm{n}}$). This means that the moment the first civilisation develops, almost all other stars is in the second index state. This provides high probabilities for the civilisation to find close encountering stars to colonize. Since the civilisations are allowed to spread to unlimited amount of close encounters each time step, the spread increases exponentially which leave few planets for the late-developing civilisations to colonize. In general, since there are more planets available to colonize for the early civilisations, they become dominant.

Figure 4.10 shows the degree of which the galaxy becomes dominated by only allowing a single civilisation to spread and colonize planets compared to planets only developing stationary civilisations. The civilisation that can spread between planets is seen as $N_{\mathrm{spreading}}$ while the planets with a stationary civilisation is seen as $N_{\mathrm{stationary}}$. If $N_{\mathrm{spreading}}/N_{\mathrm{stationary}} > 1$, the single civilisation is dominant, hence, has colonized more planets than there exists planets with stationary civilisations. Studying the graph where $N = 0$, the single civilisation is never dominant in the fraction. This can be explained by studying the screenshots from the animation in Figure 4.11. We can see that excluding the steepness parameter makes the index 2 stars jump very quickly up to index 3. This means that there is very little time for the single civilisation to meet close encountering index 2 stars. By this mean, the number of stars "naturally[7]" reaching evolution index 3 begins to dominate. Note that the single civilisation is not allowed to spread to stars already stationary colonized. Studying Figure 4.11.b, it can be seen that there are very few index 2 stars in comparison to index 3 stars. After ~ 12 Gyr almost all of the planets are inhabited by stationary civilisations where only 3 out of the 1000 planets, 4 out of the 600 planets, and 2 out of the 200 planets are colonized by the single civilisation.

For $N = 3$ however, the results are different. Indeed, for 200 and 600 stars, the stationary civilisations still dominate having ~ 85 per cent of the planets colonized for 200 stars and ~ 66 per cent for 600 stars at the end of the simulation. For 1000 stars, the single civilisation becomes the dominant since there are enough close encountering index 2 stars for the civilisation to spread to. When studying Figure 4.12 (despite it showing less stars with a much larger time step), the transition time between indices of stars is much shorter in comparison to Figure 4.11 due to the included steepness parameter. Since all stars have reached index 2 at the time when the first civilisation develops, the chance of them finding a close encountering star is large, because the large number of stars considered makes the mean distance between the stars to be small. As the number of stars increases, also the mean distance between the stars decreases and the probability for the single civilisation to encounter a close enough star grows.

In Figure 4.11, an animation over the spreading of a single civilisation can be seen where the different colors and symbols change according to Table 2.1. Here, N in equation (2.3) is set to zero. Note that the first index 3 stars (and also the first

[7]Naturally means the stars which have developed a stationary civilisation and not been colonized by another civilisation.

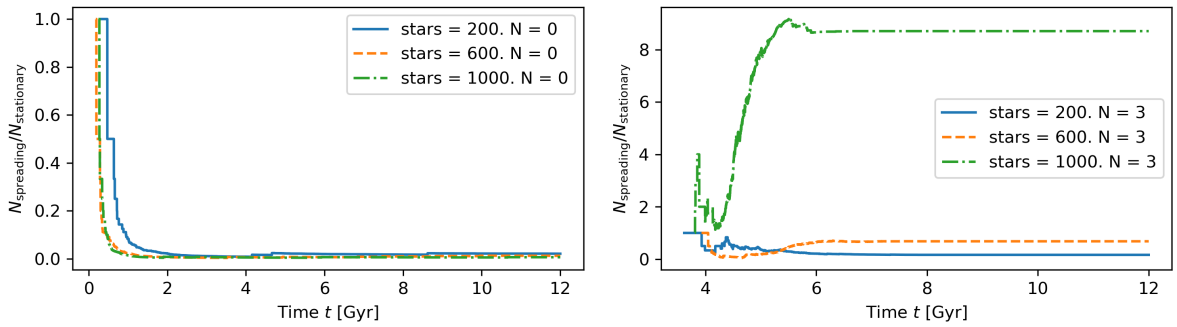

Figure 4.10: The graph illustrates the fraction of planets colonized when only a single civilisation is able to travel between stars, while the other civilisations stay stationary on their home planets. $N_{\text{spreading}}$ describes the planets colonized by the single civilisation and $N_{\text{stationary}}$ are the planets colonized by stationary civilisations. The left plot displays the fraction for 200, 600 and 1000 stars for steepness parameter $N = 3$ and the right shows this for $N = 0$. Note that if $N_{\text{spreading}}/N_{\text{stationary}} > 1$, the single civilisation dominates. It can be seen that only for 1000 stars with $N = 3$, the single civilisation has colonized more planets than there are planets with stationary civilisations. The convergence seen in the graphs is when there are no more planets to colonize, hence, when every star has reached evolution index 3. Note that the simulation in the right panel begins at time ~ 3 Gyr. This is the time when the first civilisation has developed.

civilisations, seen as navy blue in Figure 4.11.b) evolves at roughly time = 100 which for this animation is approximately 240 Myr (dt = 2.4 Myr). The spread of indices propagates until all stars have reached this level. After $\sim$ 9.6 Gyr, the first colonization of planets by the traveling civilisation happens and continues to 5 planets after the total time of 12 Gyr. Note the large time step of 2.4 Myr which makes the somewhat animation unrealistic. The optimal time step of 0.1 Myr would yield more spreading between stars in a shorter time since none of the close encountering stars would be overlooked. Due to limited computing power, this could not be achieved, however, it still works well for illustrating motion of stars, show how the planets evolve and to see how a civilisation spreads between planets.

An inclusion of the steepness parameter $N = 3$ can be seen in Figure 4.12. The animation shows clear transition times between the indices. In comparison to Figure 4.11, every star reaches a certain evolution index before increasing to the next. This is a direct result of the manipulation of the Poisson distribution where a larger N makes the probability of transition times increase as $t - t_0 \longrightarrow T_{\text{n}}$. The first index 1 stars are found after $\sim$ 600 Myr, where all of the stars have reached this state after $\sim$ 1.8 Gyr. Index 2 stars have started to evolve on the 2.4 Gyr mark and reached its maximum at 3.6 Gyr. This is in close coherence with the values of Table 2.1, where the oxygen development process takes $\sim$ 3.9 Gyr. After 7.4 Gyr, all stars have reached index 3 and after 12 Gyr, the civilisation has spread to 7 planets.

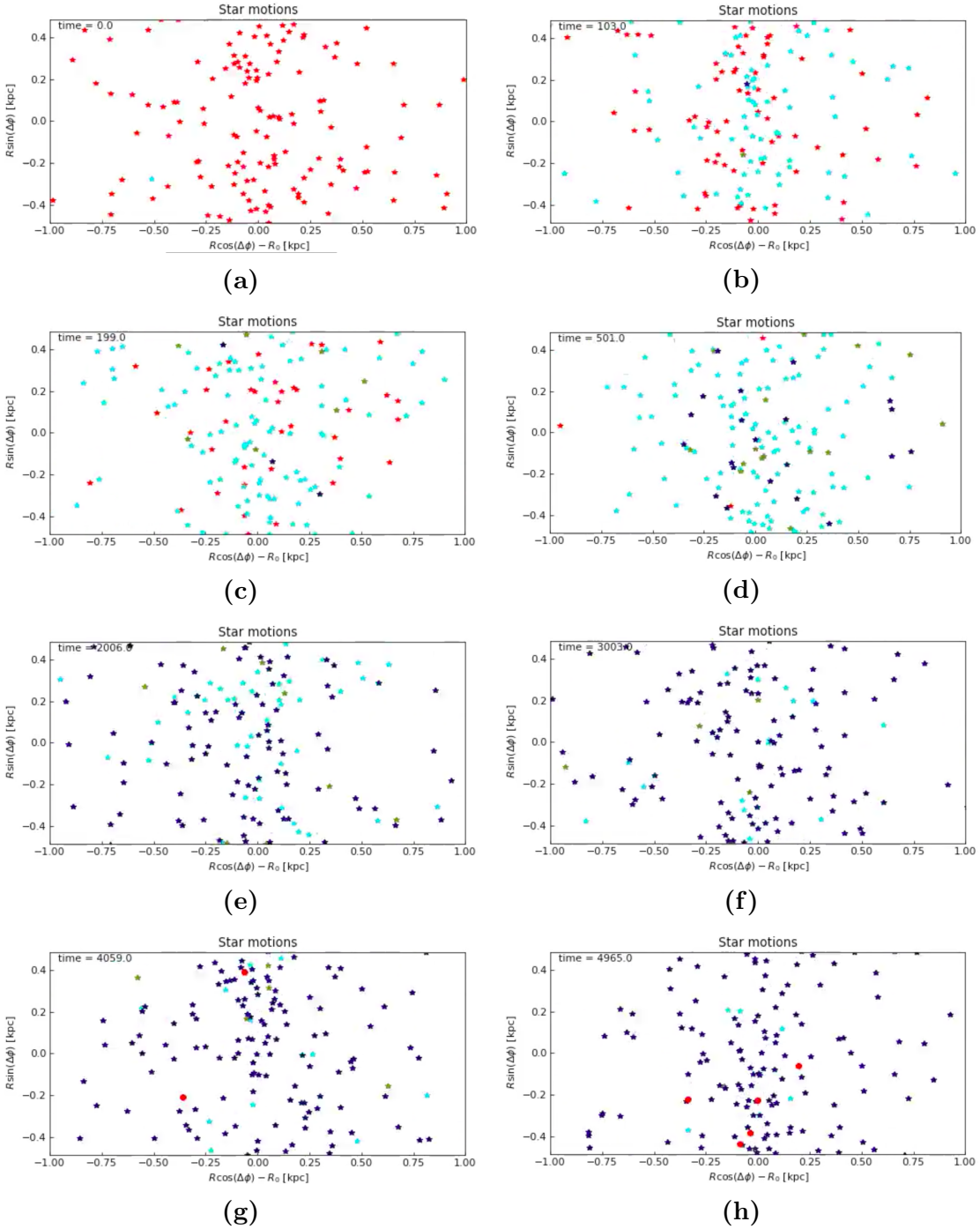

(a) (b) (c) (d) (e) (f) (g) (h)

Figure 4.11: An illustration over the evolution of indices for 200 stars and the colonization of the first developed civilisation. Index 0 stars are seen as red stars, index 1 stars as light blue, index 2 stars as olive green, index 3 stars as navy blue and the colonized stars by one civilisation are seen as red circles. The steepness parameter is set to $N = 0$. The time stamps of the screenshots are chosen to illustrate the times of transition, thus, when most of the stars increase in index. The time step used is $\mathrm{d}t = 2.4$ Myr and the time of the simulation is set to 12 Gyr.

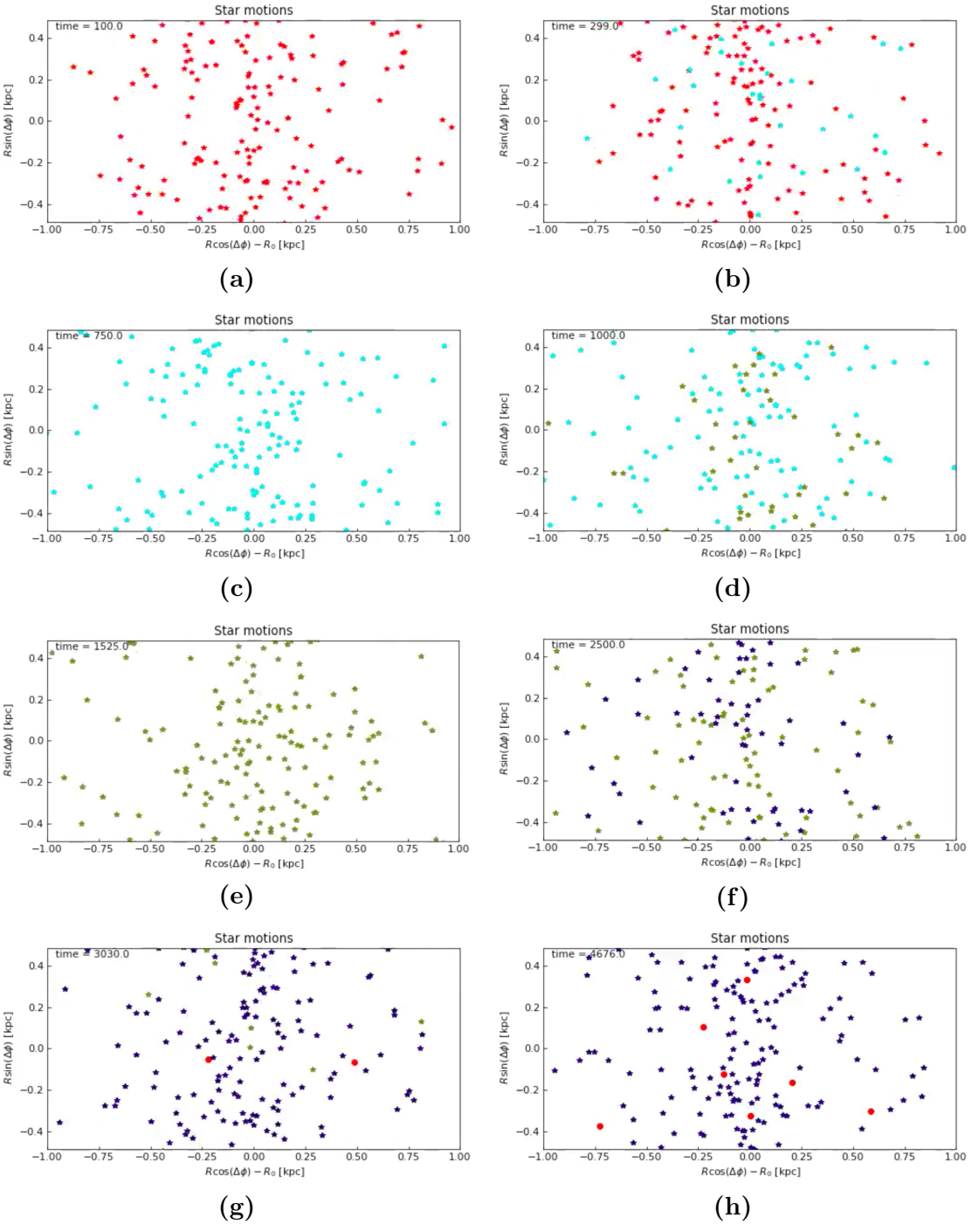

Figure 4.12: An illustration over the evolution of indices for 200 stars and the colonization of the first developed civilisation. Index 0 stars are seen as red stars, index 1 stars as light blue, index 2 stars as olive green, index 3 stars as navy blue and the colonized stars by one civilisation are seen as red circles. The steepness parameter is set to $N = 3$. The time stamps of the screenshots are chosen to illustrate the times of transition, thus, when most of the stars increase in index. In comparison to figure 4.11, there is very little mixing between the indices. This is a result from the included steepness parameter which narrows the probability distribution, making the chance of index increase small for times smaller than the process times T_{n}. The time step used is $\mathrm{d}t = 2.4$ Myr and the time of the simulation is set to 12 Gyr.

Chapter 5

Discussions and conclusions

Realism, parameters and simulation results

To begin with, a successful representation of civilisations spreading across the galaxy was obtained with several implied results such as the number of planets colonized, the number of close encounters, and indices of star states in their evolutionary process. The key parameters realized were the limit distance r_{t}, and the process times T_{process}. These parameters must be chosen to represent "realistic" values, despite their high uncertainty. Space travel between stars has so far only been theoretically tackled and the times to reach sub-relativistic travel speeds might be further or closer into the future than one might think. The process times for index increase is based on the abiogenesis (life development) of Earth. Other celestial objects or systems might have completely other time scales and parameters for technological civilisations to evolve. Many new systems with potentially habitable conditions are for example found around M dwarfs, where the habitable zone lies closer to the host star than on Earth (see Gillon et al. 2016). A planet closer to the star can imply higher sources of radiation which could increase the time of organic development since it is, for the majority of organisms, harder to adapt to radioactive environments. At the same time however, since dwarf stars live significantly longer than sun-like stars (Bertulani 2013), they also have longer time to develop habitable conditions.

The uncertainties were tackled by introducing probabilities for the evolution process of the stars, increasing their time intervals for undergoing its evolutionary processes. One can here conclude that probabilities chosen without any steepness parameter change the planets evolutionary time scales to be unlike Earth's, while the manipulation of the steepness parameter N, described in section 2.2.2, directs the theory towards Earth's uniqueness and that general life development happen according to how life evolved here.

The comparison by planets colonized by a single spreading civilisation and multiple stationary civilisations is seen in Figure 4.10. This shows that only for 1000 stars with steepness parameter of $N = 3$, a single spreading civilisation dominates the galaxy in comparison to several stationary civilisations. It is important to note that the mean distance between stars, in this case, is smaller than for 600 and 200 stars.

This increases the probability for the single civilisation to find close encountering index 2 stars as they develop. The steepness parameter makes the transition times between indices narrower. Every star has reached the state of index 2 before any of them increases to index 3. Since the single spreading civilisation is chosen to be the one on the first developed index 3 star, it means that in the first time step, the majority of other stars are index 2 stars. Due to the smaller mean distance between stars when considering 1000 stars, many of them become close encountering stars to the civilisation. This means that the civilisation can start to spread almost instantaneously. Once they have colonized a few planets, the number of planets they can colonize increases exponentially, with an increase occurring faster than the naturally developing stationary civilisations. This shows how different the outcomes can be by only varying the number of stars included.

Despite that the single spreading civilisation is dominant in the galaxy for 1000 stars, the mean distance between stars with habitable planets is still significant. Examining 1000 stars, the mean separation is 36 pc which would - for a civilisation traveling with fusion engines - take at least 150 years to travel to. This can be one of the limiting factors to why civilisations choose not to spread across the galaxy, since they would have to rely on waiting for close encountering stars before they can travel.

Limitations and assumptions

It is important to note the assumptions made throughout the project. The epicycle approximation is one (discussed in Appendix B), together with assumptions regarding the civilisations and number of stars considered. The simulation was done with a maximum of 1000 stars to reduce the computing time, but would optimally be chosen from some real measurement of the average number of stars in the habitable zone contained in a section of volume around the solar neighborhood as large as in this project. Also, every civilisation is assumed to develop the same way, being technical enough for space travel. Realistically, the development of civilisations on the planets could be different, perhaps making only a fraction of them able to travel. A more involved analysis could incorporate the ability for a civilisation to colonize planets with lower indices than 2. Since the civilisation is assumed to be technologically developed, they could potentially develop techniques to survive in conditions that is considered non-habitable as they evolve. As the civilisations develop, they might invent ways to survive on a planet with e.g. lower oxygen levels compared to Earth which in turn yields more possible planets to colonize.

Improvements and extension of the project

Improvements in the simulation would regard increasing the number of parameters considered. Optimally, the switching between indices could be changed to some more intricate model of how abiogenesis could develop differently depending on the location, structure, and chemical composition of the system. This would also imply the extension of adding other types of stars than sun-like stars, perhaps considering potentially habitable exoplanets recently found. However, since the simulation

considers the Milky Way galaxy, we would still have the constraint of choosing stars located in the solar neighborhood in our galaxy since the Milky Way potential is used to derive the motion of the stars.

Philosophical viewing points

The Fermi's paradox may be a result of ethics; a civilisation with sufficient technology for space travel may not need to travel between stars. If ramjet fusion engines are used, giving traveling speeds up to 77 % of the light speed (Kaku 2008), it would still take at fastest ~ 35 years to reach an average distant close encountering star of 7.6 pc (without the concern of matching orbits when landing or travel fuel-efficiently) which might be a big constraint when considering space travel. If a lower limit radius would be chosen for the civilisation, the times of travel would decrease but also the stars falling into the category of being close encounters would decrease. By virtue of the ethical aspect, extra-terrestrial life may not have been found by the reason that they do not want to be found. Dissimilar to us on Earth, perhaps they are not interested in the search for other life forms.

Conclusions

Using the epicycle approximation throughout the simulation yielded a useful model of the motion of stars in the introduced section around the solar neighborhood. The near-circular motion of stars in the galactic potential showed that stars tend to oscillate around their guiding center with approximately a 2:1 ratio radially compared to vertically. Using the motion of stars to find all stars counting as close encounters, thus, have a separation distance of less than 10 pc, 0.6 per cent of all possible pairs of stars where classified as close encounters. However, the motion of stars simulated are assumed not to be affected by the evolution of the galaxy itself, which if included could alter their orbits over time and change the number of stars counting as close encounters.

The choice of the steepness parameter N and the number of stars used in the simulation were crucial to reach several results. Changing this parameter can alter the probability distributions governing the planetary evolution's. A large steepness parameter forces the evolution of planets to happen according to the time scales on Earth, which yields more habitable planets for the first developed civilisation to colonize in comparison to planets naturally developing civilisations that stays stationary at their home planets, if the number of stars ≥ 1000. By excluding the steepness parameter, this civilisation has not enough planets available for colonization, making the stationary civilisations dominant after 12 Gyr of simulation time. By varying such - and other external - parameters, the model can be used to simulate important properties of how galactic colonisation could occur in the galaxy. If one would know relevant developing parameters in other galaxies, this simulation could help to investigate how colonization between planets in the habitable zone inside such a galaxy could happen. However, constraints such as using the epicycle approximation for the motion of stars and considering another galactic potential would still be limiting factors.

The motivation for this project was based on an interest in astrobiology and simulation development, produced from theoretical models. It has developed new perspectives concerning future chances of galaxy spread and introduced several aspects of how the patterns of evolution for civilisations could vary, depending on the system in consideration. The project sheds light on important aspects in terms of discovering extraterrestrial life in the future. This provides strong motivation for the continuation of developing and extending the project in the future.

Appendix A

Animations

This Appendix include the screenshot images together with the links for the animations made. The three first links corresponds to the screenshots seen Figure A.1 to A.4. The 2 subsequent links are animations from two other runs of the script (hence they differ a bit due to the random parameters, but uses the exact same code) with the same parameters for the galactic civilisation, but with increased quality.

The animation for close encountering stars can be seen via the following link:

- `https://www.youtube.com/watch?v=5_r0ZV6Pb3Y`

The animation for the civilisation spread can be seen via the following links:

- `https://youtu.be/dVRbFwqwDU8` for $N = 0$
- `https://youtu.be/hkC3yvGfPuI` for $N = 3$.

I recommend slowing the last two videos down to half speed since the time step used in these animations is large. You can also view the videos with higher quality in the links below.

The videos with higher quality can be seen via the following links:

- `https://youtu.be/R4FoQmKaoGk` for $N = 0$.
- `https://www.youtube.com/watch?v=BxjkVAdAWAM` for $N = 3$.

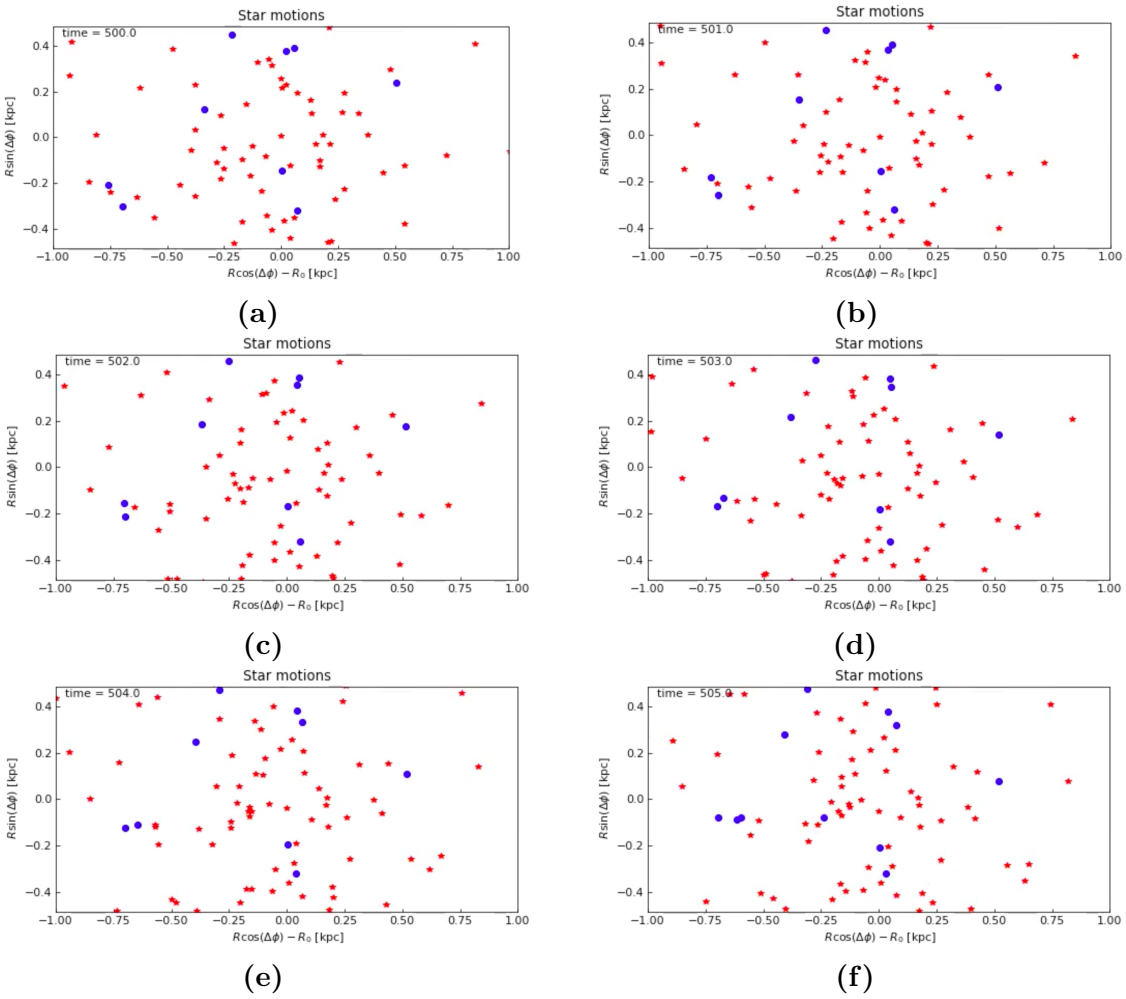

Figure A.1: A figure showing screenshots of 6 consecutive iterations for the animation of the epicycle motion of 100 stars. The purpose is to show how stars move in epicycle motion. In this simulation, 1 time unit = 1 Myr with the blue dots indicating stars that under some iteration had a close encounter. Note that the same star can be close to more than one star in the time of the simulation, which explains why there are an uneven number of stars in some screenshots. This is seen in **(b)** where one of the three stars in the first pair created, formed a new close encounter with the third star.

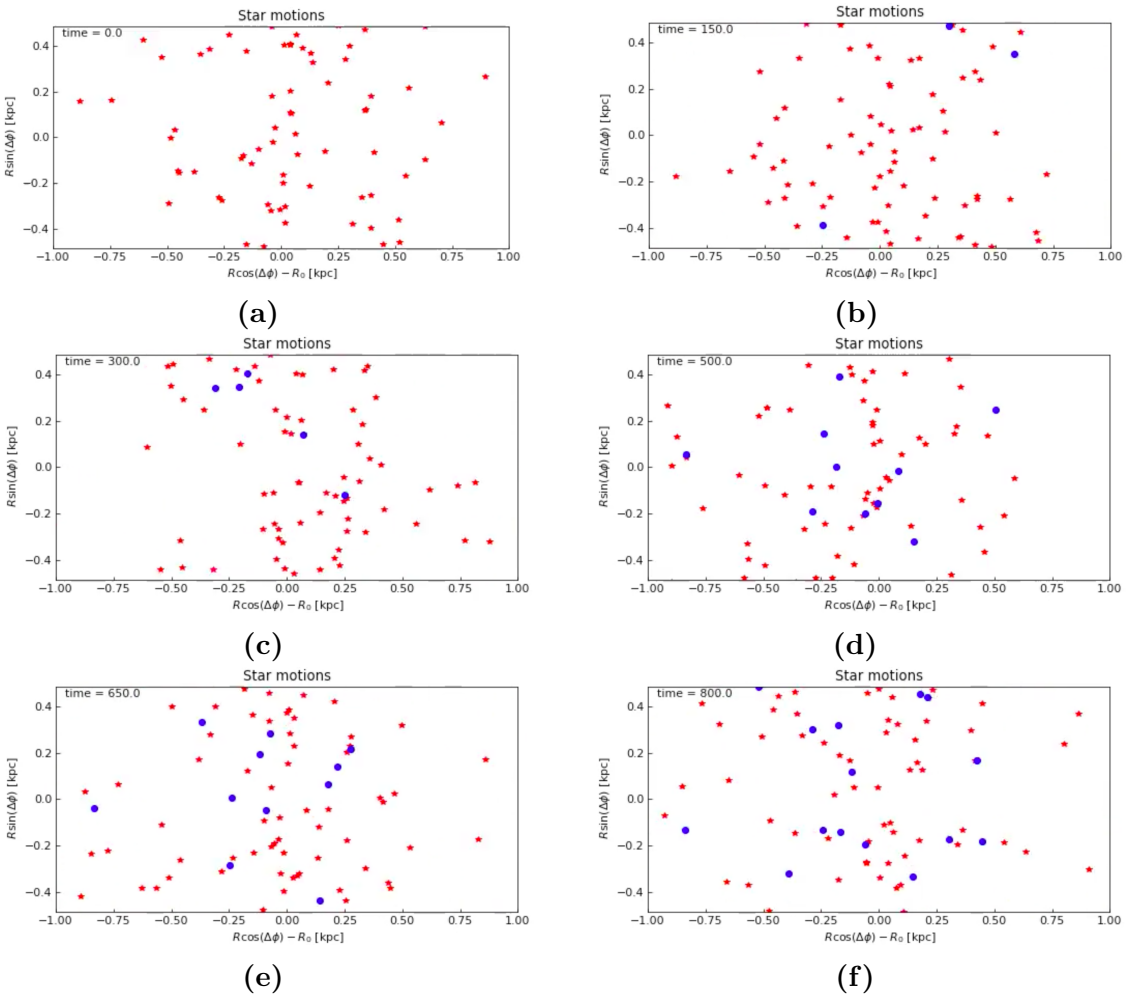

Figure A.2: A figure showing screenshots of 6 iterations for the animation of the epicycle motion of 100 stars. The purpose is to show how the number of close encounters increases over time. In this simulation, 1 time unit = 1 Myr with the blue dots indicating stars that under some iteration had a close encounter. The first close encountering stars are found after $\sim$ 150 Myr and continue to increase over time. Note that the same star can be close to more than one star in the time of the simulation, which explains why there are an uneven number of stars in some screenshots. This is seen in **(b)** where one of the three stars in the first pair created, formed a new close encounter with the third star.

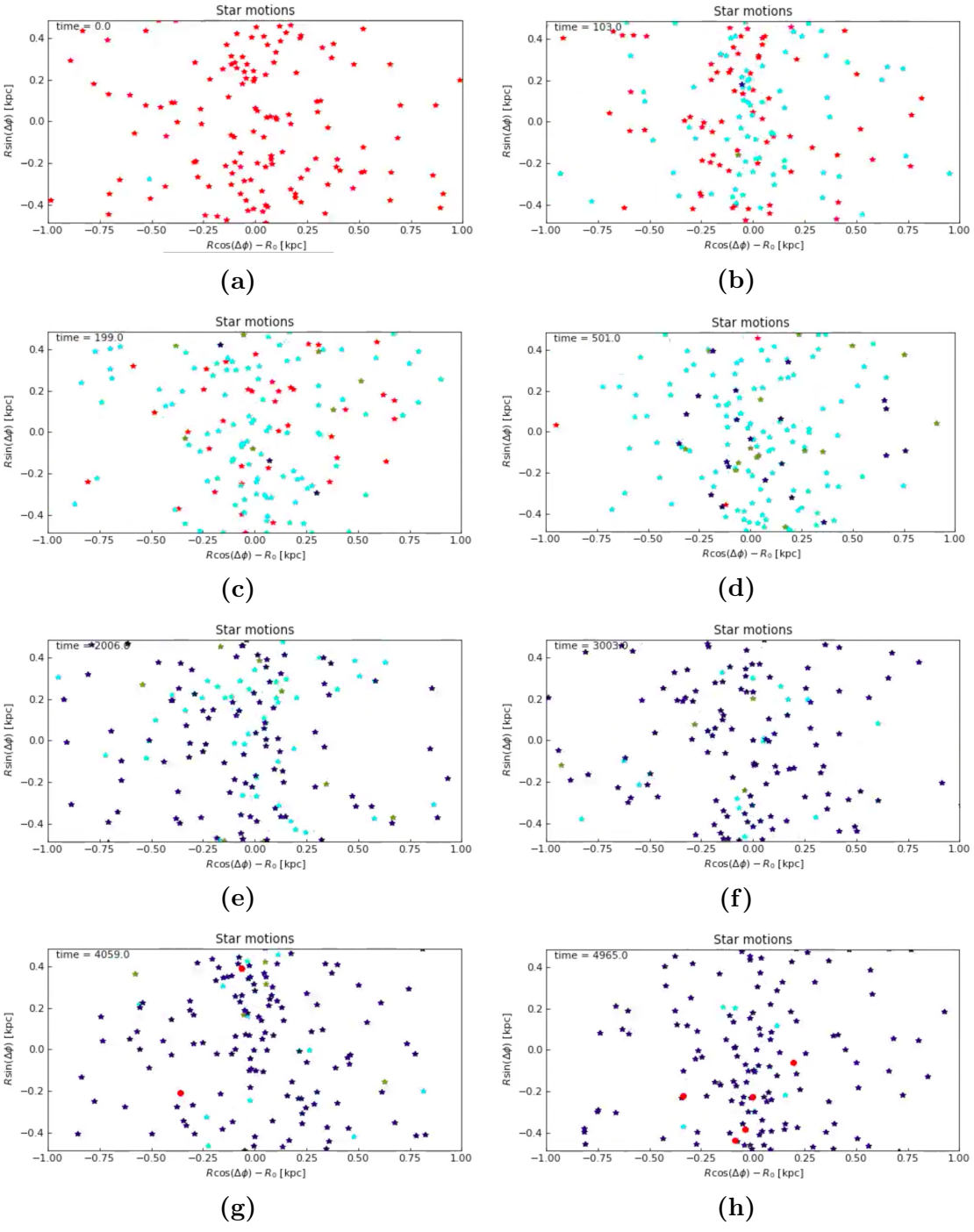

Figure A.3: An illustration over the evolution of indices for 200 stars and the colonisation of the first developed civilisation. Index 0 stars are seen as red stars, index 1 stars as light blue, index 2 stars as olive green, index 3 stars as navy blue and the colonized stars are seen as red ball shapes. The steepness parameter is set to $N = 0$. The time stamps of the screenshots are chosen to illustrate the times of transition, thus, when most of the stars increase in index. The time step used is $\mathrm{d}t = 2.4$ Myr and the time of the simulation is set to 12 Gyr.

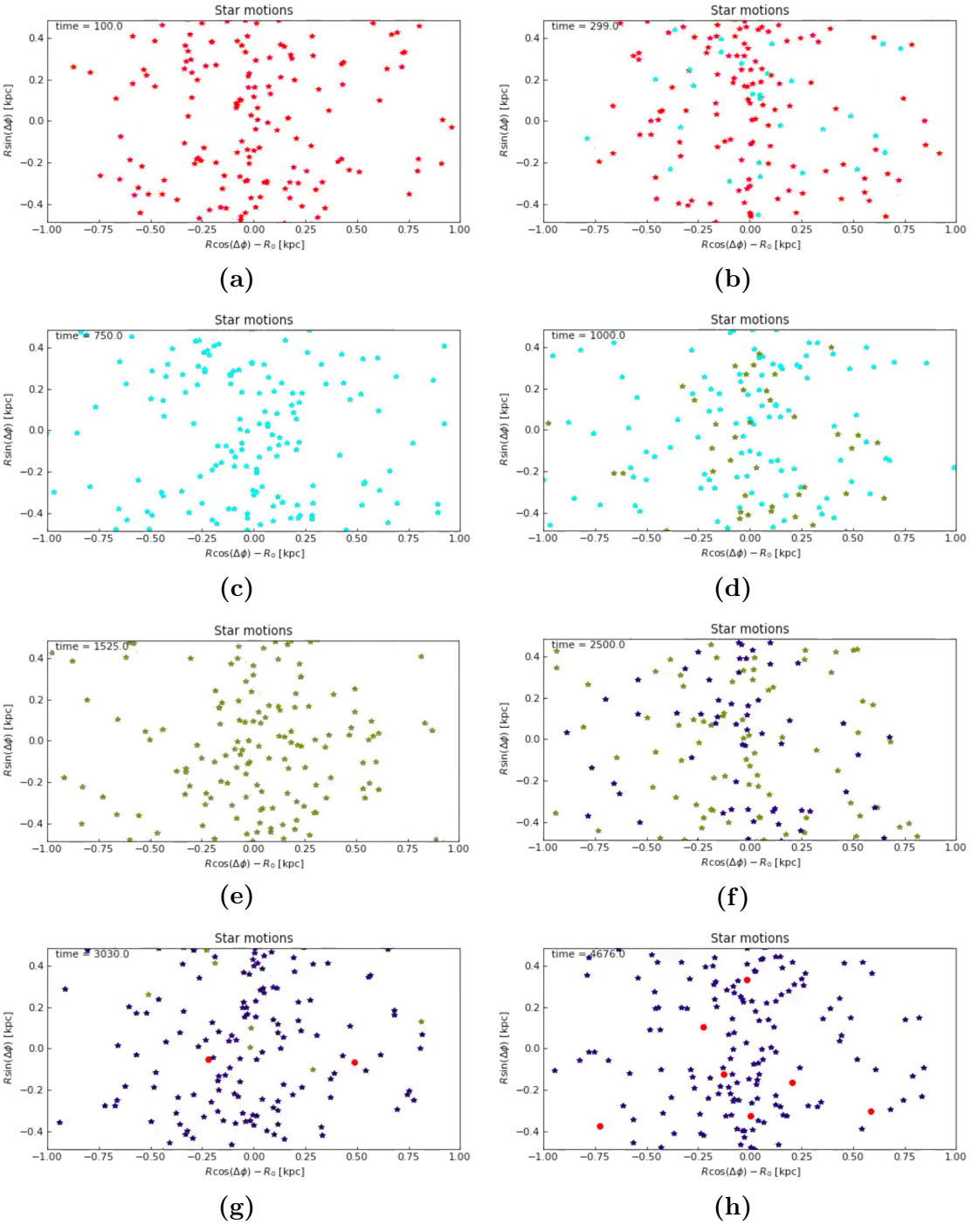

Figure A.4: An illustration over the evolution of indices for 200 stars and the colonisation of the first developed civilisation. Index 0 stars are seen as red stars, index 1 stars as light blue, index 2 stars as olive green, index 3 stars as navy blue and the colonized stars are seen as red ball shapes. The steepness parameter is set to $N = 3$. The time stamps of the screenshots are chosen to illustrate the times of transition, thus, when most of the stars increase in index. In comparison to figure 4.11, there is very little mixing between the indices. This is a result from the included steepness parameter which narrows the probability distribution, making the chance of index increase small for times smaller than the process times T_{n}. The time step used is $\mathrm{d}t = 2.4$ Myr and the time of the simulation is set to 12 Gyr.

Appendix B

Formal derivation of the epicyclic approximation

The basic derivation is based on the work in Van Den Bosch (2020, page. 1-6) and will more formally be derived here.

Assume a disk galaxy (for example the Milky Way) in cylindrical coordinates where the azimuthal motion is a function of radius and vertical distance as $\Phi = \Phi(R, z)$, following Newton's equation of motion via

$$\begin{cases} \ddot{R} - R\dot{\theta}^2 = -\frac{\partial \Phi}{\partial R} \\ \frac{d}{dt}(R^2\dot{\theta}) = 0 \\ \ddot{z} = -\frac{\partial \Phi}{\partial z} \end{cases}, \tag{B.1}$$

in cylindrical coordinates (R, θ, z). Here, $L_z = R^2\dot{\theta}$ describes the conservation of angular momentum and $-\partial\Phi/\partial R$ and $-\partial\Phi/\partial z$ describes the coupled oscillations in direction R and z. With an effective potential $\Phi_{\text{eff}} = \Phi + L_z^2/2R^2$, this can be further simplified to

$$\begin{cases} \ddot{R} = -\frac{\partial \Phi_{\text{eff}}}{\partial R} \\ \ddot{z} = -\frac{\partial \Phi_{\text{eff}}}{\partial z} \end{cases}. \tag{B.2}$$

The circular orbit of the system has a radius equal to the guiding centre $R = R_0$. For a small section around the guiding centre, the effective potential can be Taylor expanded around $(R - R_0, y) = (0, 0)$, yielding

$$\Phi_{\text{eff}} = \Phi_{\text{eff}}(R_0, 0) + (\Phi_x)x + (\Phi_y)y + (\Phi_{xy})xy + \frac{1}{2}(\Phi_{xx})x^2 + \frac{1}{2}(\Phi_{yy})y^2 + \mathcal{O}(xz^2) + ... \tag{B.3}$$

where $x = R - R_0$. By the symmetry of R_0; $(\Phi_x, \Phi_y, \Phi_{xy})|_{(R_0,0)} = 0$. The epicycle approximation holds up the second order with an effective potential defined as

$$\Phi_{\text{eff}} = \Phi_{\text{eff}}(R_0, 0) + \frac{1}{2}\kappa^2 x^2 + \frac{1}{2}\nu^2 y^2 \tag{B.4}$$

with the epicycle frequency κ and vertical frequency ν, defined as $\kappa^2 \equiv \Phi_{xx} = \partial^2\Phi_{\text{eff}}/\partial x^2$ and $\nu^2 \equiv \Phi_{xx} = \partial^2\Phi_{\text{eff}}/\partial y^2$. This yields the equation of motions in the tangential plane symmetric around $\dot{\theta}$ (meridional plane)

$$\begin{cases} \ddot{x} = -\kappa^2 x \\ \ddot{y} = -\nu^2 y \end{cases}, \tag{B.5}$$

where the x- and y motions are harmonic oscillations with the epicycle- and vertical frequencies. The circular frequency is given by

$$\omega(R) = \sqrt{\frac{1}{R}\left(\frac{\partial\Phi}{\partial R}\right)\Big|_{(R_{\text{g}},0)}} = \frac{L_{\text{z}}}{R^2}, \tag{B.6}$$

which yields

$$\kappa^2 = \left(\frac{\partial^2\Phi_{\text{eff}}}{\partial R^2}\right)\Big|_{(R_{\text{g}},0)} = \left(R\frac{d\omega^2}{dR} + 4\omega^2\right). \tag{B.7}$$

A galactic potential with a homogeneous mass distribution, $\kappa = 2\omega$ and Kepler potential, $\kappa = \omega$, for $\omega < \kappa < 2\omega$ yields the total motion as in equation (1.12), obeying

$$\begin{cases} R(t) = R_0 + a\sin(\kappa t + \varphi) \\ \phi(t) = \phi_0 + \omega_0 t + \frac{2\omega_0}{R_0\kappa} a\cos(\kappa t + \varphi) \\ z(t) = b\cos(\nu t + \varphi_z) \end{cases}. \tag{B.8}$$

Validity

The validity and derivation of the epicycle approximation is only possible considering roughly constant star density, especially in the z direction as $\ddot{z} = \nu^2 z$ must imply $\rho(z)$ to be constant. Also, by the use of a Taylor expansion around the guiding centre, the radial extension around R_0 cannot be too large. For more formal calculations, the star density should vary with R and z (and for exact calculations, also ϕ), changing the equations of motions used.

Bibliography

Anand, Mahesh et al. (2018). *An introduction to astrobiology*. 3rd ed. Cambridge University Press.

Armstrong, Stuart and Anders Sandberg (Aug. 2013). "Eternity in six hours: Intergalactic spreading of intelligent life and sharpening the Fermi paradox". In: *Acta Astronautica* 89, pp. 1–13. DOI: 10.1016/j.actaastro.2013.04.002.

Aumer, Michael and James J Binney (2009). "Kinematics and history of the solar neighbourhood revisited". In: *Monthly Notices of the Royal Astronomical Society* 397.3, pp. 1286–1301.

Bertulani, Carlos A. (2013). *Nuclei in the Cosmos*. World Scientific.

Canfield et al. (2000). "The Archean sulfur cycle and the early history of atmospheric oxygen". In: *Science* 288.5466, pp. 658–661.

Carroll-Nellenback, Jonathan et al. (Aug. 2019). "The Fermi Paradox and the Aurora Effect: Exo-civilization Settlement, Expansion, and Steady States". In: *The Astronomical Journal* 158.3, p. 117. ISSN: 1538-3881. DOI: 10.3847/1538-3881/ab31a3. URL: http://dx.doi.org/10.3847/1538-3881/ab31a3.

Cubarsi, Rafael (June 2013). "The epicycle model". In: *Modelling in Science Education and Learning* 6, p. 171. DOI: 10.4995/msel.2013.1944.

Dodd, Matthew S et al. (2017). "Evidence for early life in Earth's oldest hydrothermal vent precipitates". In: *Nature* 543.7643, pp. 60–64.

Francis, Charles (2009). *Lindblad's epicycles - valid method or bad science?* arXiv: 0911.1594 [physics.gen-ph].

Gillon, Michaël et al. (2016). "Temperate Earth-sized planets transiting a nearby ultracool dwarf star". In: *Nature* 533.7602, pp. 221–224.

Howell, Elizabeth (Apr. 2018). *Fermi Paradox: Where Are the Aliens?* URL: https://www.space.com/25325-fermi-paradox.html.

Jones, Andrew Zimmerman (May 2019). *How Stars Make All of the Elements*. URL: https://www.thoughtco.com/stellar-nucleosynthesis-2699311.

Kaku, Michio (2008). *Physics of the impossible: a scientific exploration into the world of phasers, force fields, teleportation, and time travel*. Doubleday.

Kennedy, Tom (Apr. 2020). *Pseudo-random numbers generators*. URL: https://www.math.arizona.edu/~tgk/mc/book_chap3.pdf.

Lindegren, L (2010). *Dynamical Astronomy: Lecture Notes for ASTM13*. Lund Observatory.

Lineweaver, Charles H (2001). "An estimate of the age distribution of terrestrial planets in the universe: quantifying metallicity as a selection effect". In: *Icarus* 151.2, pp. 307–313.

Makarov et al. (Aug. 2004). "Kinematics of stellar associations: The epicycle approximation and the convergent point method". In: *Monthly Notices of the Royal Astronomical Society* 352, pp. 1199–1207. DOI: 10.1111/j.1365-2966.2004.08012.x.

McMillan, Paul J (2017). "The mass distribution and gravitational potential of the Milky Way". In: *Monthly Notices of the Royal Astronomical Society*, stw2759.

Nasa (Jan. 2019). *How Old Are Galaxies?* URL: https://spaceplace.nasa.gov/galaxies-age/en/.

Oliphant, Travis E (2006). *A guide to NumPy*. Vol. 1. Trelgol Publishing USA.

Olling, Rob P and Walter Dehnen (2003). "The Oort constants measured from proper motions". In: *The Astrophysical Journal* 599.1, p. 275.

SETI (2020). URL: https://www.seti.org/drake-equation-index.

Spiegel, David S and Edwin L Turner (2011). "Life might be rare despite its early emergence on Earth: a Bayesian analysis of the probability of abiogenesis". In: *ArXiv e-prints*.

Stella, Rose (2019). "Strange Planets That Are Both Interesting And Terrifying." In: URL: https://www.boredpanda.com/strangest-weirdest-interesting-exoplanets-space/?utm_source=google&utm_medium=organic&utm_campaign=organic[Accessed%2024%20March%202020].

Van Den Bosch, Frank (Mar. 2020). *Orbits in Axisymmetric Potentials*. URL: http://www.astro.yale.edu/vdbosch/lecture6.pdf.

Virtanen, Pauli et al. (2020). "SciPy 1.0: Fundamental Algorithms for Scientific Computing in Python". In: *Nature Methods*. DOI: https://doi.org/10.1038/s41592-019-0686-2.

Zackrisson, Erik et al. (Dec. 2016). "TERRESTRIAL PLANETS ACROSS SPACE AND TIME". In: *The Astrophysical Journal* 833.2, p. 214. ISSN: 1538-4357. DOI: 10.3847/1538-4357/833/2/214. URL: http://dx.doi.org/10.3847/1538-4357/833/2/214.